Speech Attribute Detection Using Deep Learning

Ivan Kukanov

Master's Thesis

ITÄ-SUOMEN YLIOPISTO

Faculty of Science and Forestry

School of Computer Science

August 2015

UNIVERSITY OF EASTERN FINLAND, Faculty of Science and Forestry, Joensuu
School of Computing
School of Computer Science

Student, Ivan Kukanov : Speech Attribute Detection Using Deep Learning
Master's Thesis , 82 p., 3 appendix (11 p.)
Supervisors of the Master's Thesis : Dr. Ville Hautamäki
August 2015

Abstract:

In this work we present alternative models for attribute speech feature extraction based on the two state-of-the-art deep neural networks: convolutional neural networks (CNN) and feed-forward neural network with pretraining using stack of restricted Boltzmann machines (DBN-DNN). These attribute detectors are trained using data-driven approach across all languages in the OGI-TS multi-language telephone speech corpus. Thus, such a detectors can be considered as the universal phonetician alphabet (UPA), which can detect phonologically distinctive articulatory features belonging to all languages. Moreover, articulatory features can capture foreign accents characteristics and further these models will be utilized to solve the foreign accent recognition problem.

We consider two types of articulatory feature detectors, these are manner and place of articulation, which extract characteristics of the human speech production process from the speech dataset. Evaluating on the OGI-TS dataset, the results in terms of Average Equal Error Rate and Detection Error Tradeoff show that the attribute model based on the CNN consistently outperform the DBN-DNN model. Attribute detectors with CNN, versus DBN-DNN model, reduce the AvgEER producing 18.8% relative improvements for manner of articulation and producing 10.3% relative improvements for place of articulation. Also, manner speech features are detected more accurately then place features 11.46% versus 14.06% AvgEER.

Keywords:

deep neural networks, restricted Boltzmann machine, convolutional neural network, data-driven speech attributes, manner of articulation, place of articulation, foreign accent recognition

Foreword

Firstly, I would like to express my sincere gratitude to my supervisor Dr. Ville Hautamäki for the continuous support of my Master's degree study and related research, for his patience, motivation, and kindness, for giving me the opportunity to work at the Speech and Image Processing Unit. I was never bored a minute while working on several research projects over the course time. I also want to thank my reviewer Dr. Cemal Hanilci for his insightful comments and encouragement, and kindly proof-reading my thesis.

I am grateful to the whole staff of the School of Computing for help and assistance, for providing me with all the necessary facilities to implement my research projects. Special thanks to Juha Hakkarainen for his prompt response in my technical questions and requests; thanks for rebooting the GPU server while it got stuck with calculations at any time of the day or night, weekends or vacations. I thank members of our research group and colleagues, special thanks to Alexandr Sizov and Anna Fedorova for nice time spent in and out of the lab. Also thanks to my group mates of the International Master's Degree Programme in Informational Technology.

Finally, I want to thank the most valuable persons in my life, my parents Nikolay and Tatiana, and my brother Nikolay for their love and unfailing support during rough times, who encouraged me to spend time and effort on this thesis.

Joensuu September 4, 2015 *Ivan Kukanov*

List of Abbreviations

ASR	Automatic Speech Recognition
CNN	Convolutional Neural Networks
DBN-DNN	Deep Belief Neural Networks
DNN	Deep Neural Networks

Contents

CHAPTER 1

Introduction

This thesis deals with a foreign accent recognition in general and more specifically it is devoted to particular speech features which characterize different language accents. In automatic foreign accent recognition the mother tongue (L1) of non-native speakers has to be recognized given a spoken segment in a second language (L2) [31]. This task is taking much attention in the speech community because accent usually negatively affects the performance of conventional automatic speech recognition (ASR) systems [5]. The problem of the existing ASR systems that these are working mostly with the native speech only, and the accuracy dramatically reduces when words are uttered with an alternative pronunciation (e.g. foreign accent)[29]. Foreign accents also negatively affect other speech systems such as automatic speaker and language recognition [5, 4]. Moreover, foreign accent recognition plays a vital needs for border control security systems [83]. It may help officials to detect immigrants with a fake passport by recognizing actual country and region of spoken foreign accent.

The main idea why the foreign accents may be recognized is because of the deviation from the standard pronunciation and influences of language L1 on L2 [66, 85]. That is non-native speakers often tend to alter some phoneme features when pronouncing a word in L2 because they usually only partially manage its pronunciation. For example, Italians often aspirate the /h/ sound in words such as *house*, *hill* or *hotel*[85]. Another anomaly in pronunciation may be replacing an unfamiliar phoneme in L2 with the one that closer and easier to utter in L1[85]. As an example from [85], word *closely* in English can be pronounced as «k l ow s l iy», in Japanese it may has the next phonetician content «k uh l ow s l iy».

A naive solution for accent recognition could be the use of language recognition techniques based on n-gram phoneme statistics, but this approach can not be directly used, because the collected phoneme statistic would match the L2 language. The problem here is that every language has its own phone set. The solution is to create *universal phonetic alphabet* (UPA) [80]. In previous works [80, 79, 57, 77, 56] it was proposed to use speech articulatory features as the UPA.

Speech articulatory features such as manner (**fricative**, **glide**, **nasal**, **silence**, **stop**, **voiced**, **vowel**) and place (**coronal**, **dental**, **glottal**, **high**, **labial**, **low**, **mid**, **palatal**, **silence**, and **velar**) can capture language and accent variations. Experimental evidence showed their effectiveness in foreign accent recognition [32, 9].

Using universal articulatory features we can analyse the statistical model for pair L1-L2 languages. For instance, if we take English and Japanese pronunciation of word *closely* and represent it in manner attribute transcription (using mapping tables from Appendix A), for English it will be «stop gs_voiced voiced_vowel fric gs_voiced voiced_vowel» and for Japanese «stop voiced_vowel gs_voiced voiced_vowel fric gs_voiced voiced_vowel». These two transcriptions differ in one manner attribute («voiced_vowel»). Thus, gathering such a statistic about different attribute content of the pronunciations we may recognize the foreign accents or dialects.

In [8] it was proposed successful bottom-up implementation of the foreign accent recognition model based on front-end attribute detectors. The low-level detectors were modeled using artificial neural networks (ANN) with single-hidden non-linear layer and soft-max output layer. However, the baseline speech attribute front-end showed large error rate variance [80]. It was needed more advanced approach to improve the detectors' accuracy.

Further, we discuss why the deep learning approaches have been chosen. The biggest advance occurred nearly four decades ago with the introduction of the expectation-maximization (EM) algorithm for training Hidden Markov Models (HMMs), see historical review on HMM [6, 28]. With the EM algorithm, it became possible to develop speech systems using the richness of Gaussian mixture models (GMMs) [58] to represent the relationship between HMM states and the acoustic input. Despite their advantages, GMMs have a serious shortcoming [40]. Artificial neural networks trained by backpropagating have the potential to learn much better models. In fact two decades ago, it was achieved some success using ANN with a single layer of non-linear hidden units. However, there was no adequate learning algorithm for training neural networks with many hidden layers on large amount of data. Also the computer hardware performance were not sufficient to seriously challenge GMMs [40].

Over the last decade, advances in both machine learning and graphics processing unit (GPU) computation led to more efficient methods. In 2006 Geoffrey Hinton's paper work [40] made a significant impact in neural networks and turned researchers mind to this field. Since that time, it became possible to train networks with many layers of non-linear units and a very large output layers. The new study of deep learning has appeared which is a branch of machine learning based on a set of algorithms that model high-level abstractions in data by using model architectures composed of multiple non-linear transformations [25].

New deep learning algorithms led to significant advances in different areas. In some fields these even outperform human abilities: in [88] it is proposed deep learning approach which beats humans in IQ test, in [34, 47] Microsoft and Google have beat the human benchmark at image recognition of 5.1% errors. Deep neural networks (DNNs) have been successfully applied in across a range of speech processing tasks as well, such as conversational-style speech recognition [76], noise robust applications [91], multi- and cross-lingual learning techniques [62] and others. Inspired by the success of those applications, we want to explore the use of DNNs to extract manner and place of articulation attributes to be used in automatic accent recognition systems.

1.1 Goals

The main goal of the research is to improve the existing foreign accent recognition system [32]. In order to refine the whole system we have to improve components it consists of. In this thesis we will improve the front-end speech articulatory detectors. For that problem the next tasks will be solved:

- implement a model for detecting speech attributes of articulation using deep learning approaches;
- the proposed model have to satisfy the attribute paradigm [56];
- investigate performance of the proposed model and apply to the foreign accent recognition.

CHAPTER 2

Artificial Neural Networks

In this chapter we briefly consider simple neural perceptron. After that we move to the multilayer neural networks, review its training algorithm Backpropagation and its advantages and drawbacks.

2.1 Single-layer Perceptron

People and animals from day to day use their brain, eyes, ears to make decisions and train itself. When we socialize with each other we do not even think of processes of recognition in the brain we easily and automatically recognize the words of people with different voices. For human brain it is easy to recognize any objects, sounds, printed or handwritten text, we do it on the fly and subconsciously.

On the other hand, scientists studied the issues of the brain activity modeling and how it solves such a complex tasks. Firstly natural nervous system was mentioned in primitive understanding by René Descartes in XVII century [30]. In his work, Descartes firstly proposed the existence of human reaction on the external events, it was the first steps of the founding of reflex theory.

In the modern understanding nervous system was described in works of Camillo Golgi and Santiago Ramon y Cajal. They got the Nobel Prize in Physiology or Medicine in 1906 «in recognition of their work on the structure of the nervous system» [1]. These study made the ground theory of the natural neural networks and moder biology.

Later on these understandings of biological neural networks mathematical *artificial neural network* (ANN) approach emerged. Artificial neural networks are mathematical models which have extremely simplified analogues of natural neural networks. But even using just a basic principals of biological neural systems it is enough to successfully solve some practical problems.

McCulloch-Pitts Neural Network Model. Let given X is a general space of objects and Y is a space of responses, there is relation $y^* : X \to Y$ which we know only on training subset of objects $X^l = (x_i, y_i)_{i=1}^l$, $y_i = y^*(x_i)$. We need to develop algorithm $a : X \to Y$ which will approximate objective function y^* on the whole space of objects X. This is a basic problem of machine learning. Further, let consider that objects can be described by n features $f_j : X \to \mathbb{R}$, $j = \overline{1, n}$, or in vector form $(f_1(x), \ldots, f_n(x))^T \in \mathbb{R}^n$.

First neural network was proposed by Warren McCulloch and Walter Pitts in 1943 [61]. It was simple linear perceptron, see Figure 2.1.

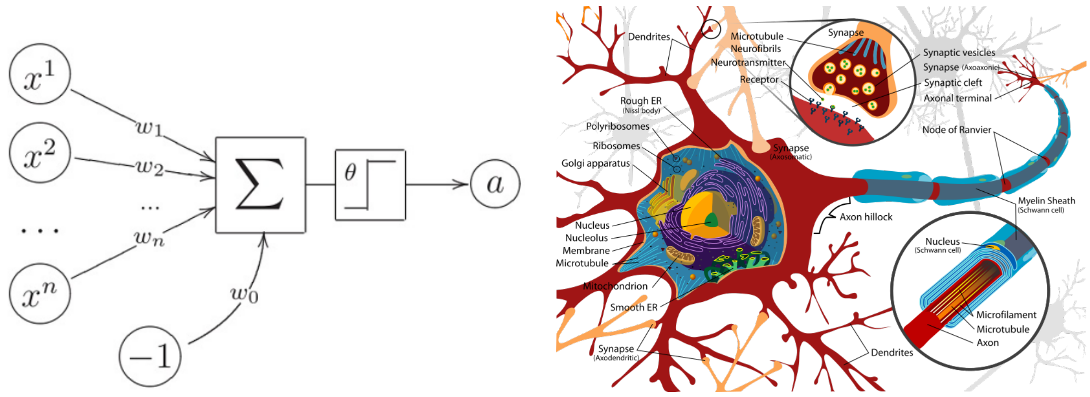

Figure 2.1: Perceptron model of Warren McCulloch and Walter Pitts and biological neural cell [90].

This model get n-dimensional feature vector as the input

$$x = \left(x^1, \ldots, x^n\right)^T \equiv (f_1(x), \ldots, f_n(x))^T,$$

here object x identified with its feature vector. For simplicity features are supposed to be binary. These features are multiplied on the respective weights $w = (w_0, \ldots, w_n)^T$. The neuron's output is 0 or 1, it is determined by the weighted input sum. If sum $\sum_{j=1}^{n} w_j x^j$ is greater then threshold w_0 then neuron is *activated* and output 1, otherwise 0. In mathematical terms it means the output from the neural network is $a(x)$:

$$a(x) = \sigma\left(\sum_{j=1}^{n} w_j x^j - w_0\right), \tag{2.1}$$

where $\sigma(z)$ is an activation function. In perceptron model activation function is a simple Heaviside step function:

$$\sigma(z) = \theta(z) = [z \geqslant 0] = \begin{cases} 0, & z < 0, \\ 1, & z \geqslant 0 \end{cases} \tag{2.2}$$

McCulloch-Pitts model is equivalent to the linear step classifier. Later perceptron model was extended to the neural networks with real value inputs and outputs and with different activation functions.

Activation functions. There are different types of neural activation functions, the choice of them depends on the practical task. Commonly used activation functions are shown on the Figure 2.2. Sometimes neurons are called regarding its activation function.

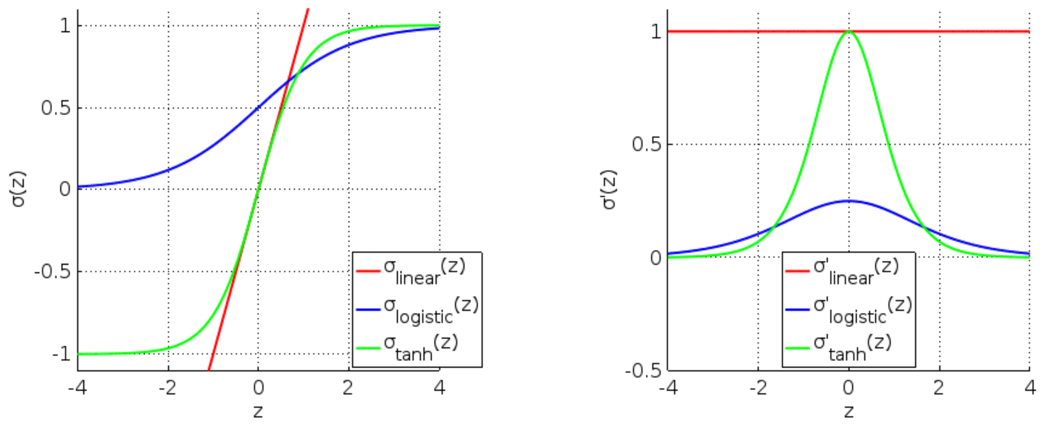

Figure 2.2: Linear, logistic and hyperbolic tangent functions and their derivatives.

Binary threshold neurons [93] which is described above, it is another name for McCulloch-Pitts model. *Linear neurons* [93] is the simplest kind of neurons. It has linear activation function

$$\sigma_{linear}(z) = z. \tag{2.3}$$

Hence, we have connection of neural networks with the linear regression model

$$a\left(x\right)=\sum_{j=1}^{n}w_jx^j-w_0=w^Tx. \tag{2.4}$$

It is computationally limited because the superposition of such neurons in many layers still gives linear model. *Sigmoid neurons* produces real valued outputs that is bounded between 0 and 1. This kind of neurons is very frequently used in neural nets

$$\sigma_{logistic}\left(z\right)=\frac{1}{1+e^{-z}}. \tag{2.5}$$

Hyperbolic tangent function [93] is a neuron with activation function

$$\sigma_{tanh}\left(z\right)=\tanh\left(z\right)=\frac{e^z-e^{-z}}{e^z+e^{-z}}. \tag{2.6}$$

Linear (2.3), sigmoid (2.5) and hyperbolic tangent (2.6) activation functions are smooth and differentiable (see Figure 2.2). Moreover, these derivatives are either constant or defined in terms of the original function

$$\begin{aligned}&\sigma'_{linear}\left(z\right)=1\\&\sigma'_{logistic}\left(z\right)=\sigma_{logistic}\left(z\right)\left(1-\sigma_{logistic}\left(z\right)\right)\\&\sigma'_{\tanh}\left(z\right)=1-\sigma^2_{\tanh}\left(z\right)\end{aligned} \tag{2.7}$$

It is a key feature that makes training very efficient and convenient for implementation of the ***Back-propagation approach*** (see later in the Section 2.3).

Rectified linear neurons (ReLU) [93] combines the ideas of both previous binary threshold and linear neurons. Firstly, it computes weighted sum of its inputs, as usually, and then it produces output of non-linear activation function

$$\sigma\left(z\right)=\begin{cases}z, & if\ \ z>0,\\0, & otherwise.\end{cases} \tag{2.8}$$

So, above zero it is linear and at zero it makes a «hard» decision.

2.2 Multi-layer Neural Networks

Computer scientists went further and again inspired by the human brain. Similarly the natural neurons works together and have difficult multilayer structure, mathematicians brought this idea to the artificial multilayer neural networks.

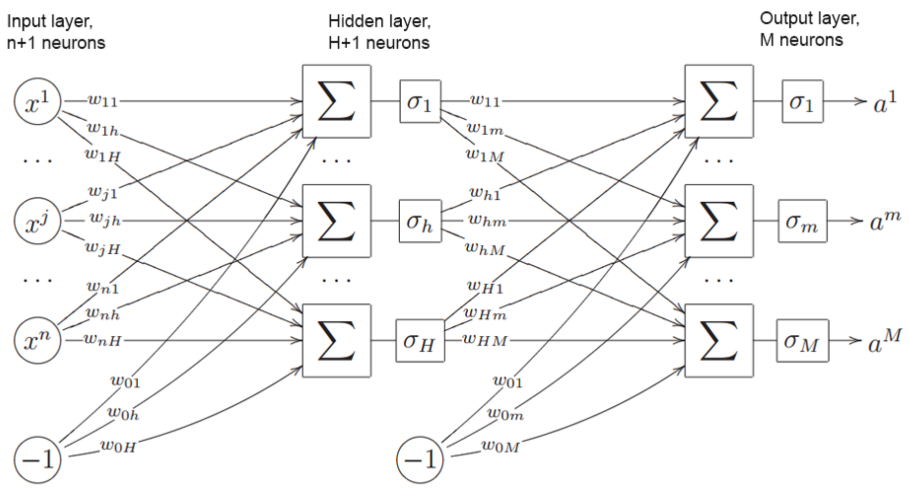

Figure 2.3: Multi-layer neural network with one hidden layer [87].

On the Figure 2.3 it is represented multilayer network with one hidden layer for simplicity. On the input layer we send n-dim feature vector, then these features simultaneously goes to the H neurons of the first hidden layer. On the hidden layer we acquire weighted sum of the features which goes through the activation function. After that it moves to next layer and so on.

On the output we get signals a^m. In general case neural networks can have arbitrary number of neurons in hidden layers and hidden layers itself. Number of output signals usually corresponds to number of classes in classification problem.

Properties of multilayer networks. The main question for machine learning is what kind of function neural networks can approximate? Here we list some features on neural networks which answer this question [33].

- Any boolean function (disjunctive normal form) can be represented by 2-layers artificial neural network in $\{0, 1\}^n$ space. It means if input features are binary and we are solving binary classification problem then it is enough to have 2-layers to approximate any boolean function [33].

If input features are not binary but real values, i.e. can neural networks approximate any continuous function? The answer to this question is embodied in the *Universal Approximation Theorem* for a nonlinear input-output mapping proved by George Cybenko [22]. This result was acquired based on the solution to the Hilbert's 13-th Problem given by A.N. Kolmogorov [48].

Theorem 1. ***(The Universal Approximation Theorem [33])*** *Let $\varphi(\cdot)$ be a nonconstant, bounded, and monotone increasing continuous function. Let I_N denote the N - dimensional unit hypercube $[0,1]^N$. The space of continuous functions on I_N is denoted by $C(I_N)$. Then, given any function $f \in C(I_N)$ and $\epsilon > 0$, there exist an integer M and sets of real constants α_i, b_i and w_{ij}, where $i = 1, \dots, M$ and $j = 1, \dots, N$ such that we may define*

$$F(x_1, \dots, x_N) = \sum_{i=1}^{M} \alpha_i \varphi\left(\sum_{j=1}^{N} w_{ij} x_j + b_i\right), \tag{2.9}$$

as an approximate realization of the function $f(\cdot)$; that is

$$|F(x_1, \dots, x_N) - f(x_1, \dots, x_N)| < \varepsilon$$

for all $x_1, \dots, x_N$ that lie in the input space.

This theorem is directly applicable to perceptron model. But the theorem does not say optimal number of neurons that should be in the neural network to perform the function approximation, it says only that it is finite number.

- With the help of linear algebraic operations and one nonlinear activation function σ we are able to approximate any continuous function with desirable accuracy [33].

- More layers neural network has then more complex decision making and more complex loss function surface it produces [33].

2.3 Training approaches

In 1949 the neuropsychologist Donald O. Hebb developed the theory of the relationship of the brain and cognitive processes [35]. In his works he described some ideas of artificial neural network structuring and layers composition. Hebb proposed hypothetical ideas of neural networks training which made up the ground theory of all nowadays neural network algorithms, commonly known as «Hebb's postulate» [33]. These are the next:

1. if two neurons from different sides of synapse are activated simultaneously, then synapse «weight» is increasing;

2. if two neurons from different sides of synapse are activated asynchronously, then synapse «weight» is decreasing or synapse is removed.

In 1958 Frank Rosenblatt, inspired by the works of McCulloch, Pitts and Hebb, developed Rosenblatt's Perceptron [70]. It was shown that perceptron can perform basic logical operations (conjunction and disjunction) and has the convergent learning algorithm (*perceptron convergence theorem* [33]). The Rosenblatt's Perceptron power is limited it can be applied only for linearly separable classes [33].

After Marvin Minski critical book about the perceptoron model [63] the interest to the neural networks was dramatically reduced. He analyzed mathematical inconsistency and limitations of the perceptron model (XOR function problem, see Figure 2.4).

The interest to the neural networks was refreshed after developing the *Error Backpropagation* algorithm by D.E. Rumelhart, G.E. Hinton and R. J. Williams in 1986 [71].

Error Backpropagation. Consider Figure 2.3, we are given $X = \mathbb{R}^n$ features and $Y = \mathbb{R}^M$ corresponding vector of responses. In our simple case one-hidden layer of neural network has $[H(n+1) + (H+1)M]$ unknown parameters (vector of all weights w) which we have to fit using training set. Usually the complexity of problem increases proportionally with the number of unknown parameters (when we add new layers). But in neural networks we can avoid this issue using efficient gradient method *error backpropagation*.

Let output layer contains M neurons with activation functions σ_m and outputs a^m, $m =$

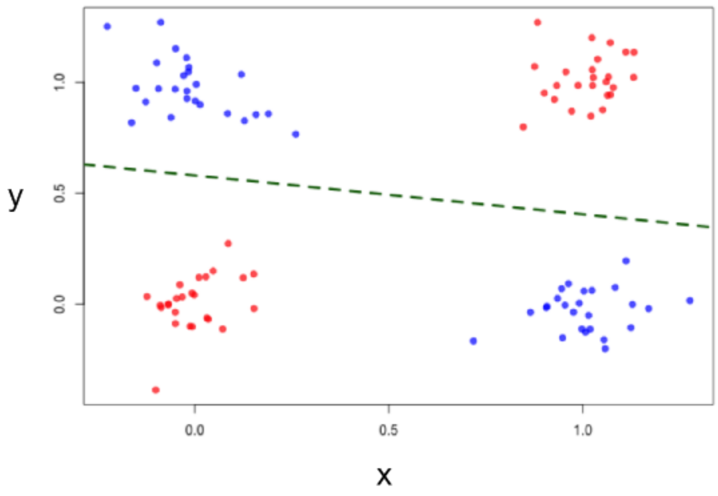

Figure 2.4: Limitations of the Rosenblatt's Perceptron, XOR function problem.

$1, \ldots, M$ signals; hidden layer has H neurons with activation functions σ_h and outputs u^h, $h = 1, \ldots, H$ signals. Weights between the neurons from the hidden layer and the output layer are denoted as w_{hm}. Weights between the input layer neurons and the hidden layer are denoted as w_{jh}.

The output signals a^m after the features x_i (i-th object features from the training set) pass through the all layers are calculated as superposition of output signals on intermediate layers:

$$a^m = \sigma_m \left(\sum_{h=0}^{H} w_{hm} u^h \left(x_i \right) \right); \quad u^h \left(x_i \right) = \sigma_h \left(\sum_{j=0}^{n} w_{jh} x_i^j \right), \tag{2.10}$$

where x_i^j is the j-th component of the i-th object feature vector.

The problem of weights training is the next we have to minimize the value of the loss function on the training set (x_i, y_i) of size l:

$$Q\left(w\right) = \sum_{i=1}^{l} \mathcal{L}\left(w, x_i, y_i\right) \to \min_{w}. \tag{2.11}$$

Popular distance measures can be used for the loss function. For the regression task [93], the *mean square error* (MSE) criterion is typically used,

$$\mathcal{L}_{MSE}\left(w, x_i, y_i\right) = \frac{1}{2} \left\| x_i - y_i \right\|^2. \tag{2.12}$$

For the classification task, where y_i is a response (probability distribution) on the i-th object and the *cross-entropy* (CE) criterion

$$\mathcal{L}_{CE}\left(w, x_i, y_i\right) = -\sum_{m=1}^{M} y_i^m \log\left[\nu^m\left(x_i\right)\right], \tag{2.13}$$

where $y_i^m = P_{emp}\left(m|x_i\right)$ is the empirical (observed in the training set) probability that the object x_i belongs to class m, and $\nu^m\left(x_i\right)$ is the same probability estimated from the DNN

$$\nu^m\left(x_i\right) = P_{DNN}\left(m|x_i\right) = \operatorname{softmax}_m\left(z_i^m\right) = \frac{\exp\left(z_i^m\right)}{\sum\limits_{m=1}^{M}\exp\left(z_i^m\right)}, \tag{2.14}$$

and $z_i^m = \sum\limits_{h=0}^{H} w_{hm} u^h\left(x_i\right)$ - m-th weighted signal on the final layer. For more details of softmax layer and cross-entropy criteria usage see [93], [67].

In our example for simplicity we will utilize MSE criterion. In order to minimize our cost function (2.11) we could use stochastic gradient descend to search the minimum [27] as for single percetron training. But it is difficult to calculate gradient directly using the loss function $\mathcal{L}\left(w, x_i, y_i\right)$, the complexity of such problem is in the order of $O\left(\left[Hn + HM\right]^2\right)$. With the aid of *error backpropagation* we can reduce the complexity to order of $O\left(3\left[Hn + HM\right]\right)$. The point of the *error backpropagation* is in the efficient differentiation of superposition of functions (chain rule differentiation). We effectively store intermediate results of the algorithm in the units of the neural network and then quickly calculate the total gradient.

Further for our one-hidden layer example the loss function $\mathcal{L}_i(w) = \mathcal{L}_{MSE}\left(w, x_i, y_i\right)$ proposed to be the mean square error calculated on every object x_i output signal, after forward pass:

$$\mathcal{L}_i\left(w\right) = \frac{1}{2}\sum_{m=1}^{M}\left(a^m\left(x_i\right) - y_i^m\right)^2. \tag{2.15}$$

So, we have to derive partial derivatives of the loss function $\mathcal{L}_i$ with respect to the output signals a^m of the final layer:

$$\frac{\partial \mathcal{L}_i\left(w\right)}{\partial a^m} = a^m\left(x_i\right) - y_i^m = \varepsilon_i^m \tag{2.16}$$

here we denote the partial derivative as ε_i^m, i.e. error estimation on the sample object x_i with response y_i.

Now consider derivatives of the hidden layer h with respect to their outputs:

$$\frac{\partial \mathcal{L}_i(w)}{\partial u^h} = \sum_{m=1}^{M} \left(a^m(x_i) - y_i^m\right) \sigma'_m w_{hm} = \sum_{m=1}^{M} \varepsilon_i^m \sigma'_m w_{hm} = \varepsilon_i^h, \tag{2.17}$$

this derivative we also call as «*error estimation*» ε_i^h of network on the hidden layer, $\sigma'_m = \sigma'_m \left(\sum\limits_{h=0}^{H} w_{hm} u^h(x_i) \right)$ is the derivative of the activation function calculated on the same argument as in (2.10). If sigmoid activation function is used then the derivative could be effectively calculated as $\sigma'_m = \sigma_m (1 - \sigma_m)$.

We can notice that ε_i^h is calculated using ε_i^m if we run the neural network backward and set $\varepsilon_i^m \sigma'_m$ on the output units and get ε_i^h on the input units as shown on Figure 2.5. That is why it is called *backpropagation*.

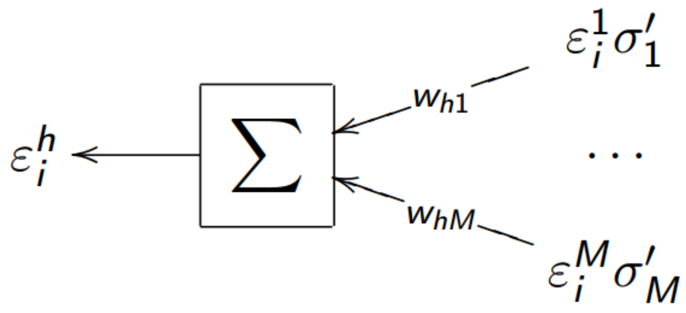

Figure 2.5: Error backward running.

When we have derivatives (2.16) and (2.17) with respect to a^m and u^h we can easily infer gradient of loss function $\mathcal{L}_i(w)$ with respect to weights:

$$\frac{\partial \mathcal{L}_i(w)}{\partial w_{hm}} = \frac{\partial \mathcal{L}_i(w)}{\partial a^m} \frac{\partial a^m}{\partial w_{hm}} = \varepsilon_i^m \sigma'_m u^h, \quad h = 0, \dots, H, \;\; m = 1, \dots, M; \tag{2.18}$$

$$\frac{\partial \mathcal{L}_i(w)}{\partial w_{jh}} = \frac{\partial \mathcal{L}_i(w)}{\partial u^h} \frac{\partial u^h}{\partial w_{jh}} = \varepsilon_i^h \sigma'_h x_j, \quad j = 0, \dots, n, \;\; h = 1, \dots, H. \tag{2.19}$$

If we have more layers then derivatives are inferred using same chain rule. Algorithm for any number of hidden layers is derived in [93].

Therefore, we have all needed information to summarize the error backpropagation for two-layer neural network in Algorithm 1.

Algorithm 1 two-layer neural network training using Error Backpropagation

```
Input: $X^l = (x_i, y_i)_{i=1}^l$ - training set, $x_i \in \mathbb{R}^n$, $y_i \in \mathbb{R}^M$;
    $H$ - number of units in hidden layers;
    $\eta$ - learning rate;
    $Q$ - loss function, initial value is calculated using equation (2.11);
    $\lambda$ - constant parameter from interval $[0; 1]$;
Output: weights $w_{jh}$, $w_{hm}$;

1: Initialisation: with small random numbers
   $w_{jh} := random\left(-\frac{1}{2n}, \frac{1}{2n}\right)$;
   $w_{hm} := random\left(-\frac{1}{2H}, \frac{1}{2H}\right)$;
2: repeat
3:     randomly choose $x_i$;
4:     forward pass:
       $u_i^h := \sigma_h\left(\sum_{j=0}^{J} w_{jh} x_i\right)$;
       $a_i^m := \sigma_m\left(\sum_{h=0}^{H} w_{hm} u^h(x_i)\right)$;
       $\varepsilon_i^m := a_i^m - y_i^m$;
       $\mathcal{L}_i := \sum_{m=1}^{M} (\varepsilon_i^m)^2$;
5:     backward pass:
       $\varepsilon_i^h := \sum_{m=1}^{M} \varepsilon_i^m \sigma'_m w_{hm}$, for all $h = 1, \dots, H$;
6:     gradient step:
       $w_{hm} := w_{hm} - \eta \varepsilon_i^m \sigma'_m u^m$,   for all $h = 0, \dots, H$, $m = 1, \dots, M$;
       $w_{jh} := w_{jh} - \eta \varepsilon_i^h \sigma'_h x^j$,   for all $j = 0, \dots, n$, $h = 1, \dots, H$;
7:     $Q := (1 - \lambda)Q + \lambda \mathcal{L}_i$;
8: until $Q$ stabilized;
```

Advantages of Error Backpropagation.

- Backpropagation is efficient algorithm, it can be easily parallelized [93].
- The algorithm is very flexible for training, i.e. it can be easily generalized on any activation functions σ and loss functions $\mathcal{L}$. Moreover, every neural unit can has its own activation function. There are no restrictions on the number of input-output units

and hidden layers. Any method of optimization can be used for training (gradient descent, conjugate gradient, the Newton–Raphson method).

Disadvantages of Error Backpropagation.

- Convergence is not guaranteed, because gradient descent tends to stuck in many local minima of the loss function $\mathcal{L}$ [93]. In order to improve convergence a lot of tricks and heuristics are used [52], [54].
- Excessive number of weight parameters w can lead to overfitting of the model [93].
- ***Vanishing gradient*** problem [44], [45]. If sigmoid or hyperbolic tangent activation functions are used then vanishing gradient problem appears. It means the larger values of weights w on the input of the unit the smaller value of the derivation σ' on the output. Therefore, weight correction on the backward pass of the backpropagation algorithm is very tiny for multi layer perceptron (more then 2 hidden layers).

CHAPTER 3

Restricted Boltzmann Machine

Vanishing gradient problem was shown in training artificial neural networks using gradient based backpropagation approaches (see [45]). Despite the tempting power of the neural networks that these are able to approximate any continuous function, it takes a lot of time to train them and there was no efficient algorithm but «tricky» backpropagation. With the advent of the backpropagation algorithm in the 1986, many researchers tried to train supervised deep artificial neural networks from scratch, initially with little success. Interest to neural networks dramatically decreased at that time and since 1992 - 2005 («period of oblivion») there were no any outstanding results in this field.

Gradient vanishing problem forced scientists to reject backpropagation algorithm and invent other approaches for training neural networks. In 2005 Geoffrey Hinton et al. suggested *unsupervised pre-training approach* [40]. It means that firstly we cluster training objects, learn generally useful feature detectors, and only after that we name that clusters, i.e. by supervised backpropagation we classify the data.

The deep model of Geoffrey Hinton involves learning the distribution of a high level representation using successive layers of binary or real-valued latent variables. It uses a restricted Boltzmann machine [82] to model each new layer of higher level features.

3.1 Notes from statistical physics

Before we go deeper into the Boltzmann Machine it would be correctly to mention what is the ground behind this techniques.

Further we remind Boltzmann distribution from statistical mechanics [49]. Let's imagine some mechanical system with many degrees of freedom, e.g. in statistical physics particles of ideal gas are considered as such system. This system can be in one of the many states with some probability p_i of that state i. Some energy E_i of the whole mechanical system corresponds to that state i.

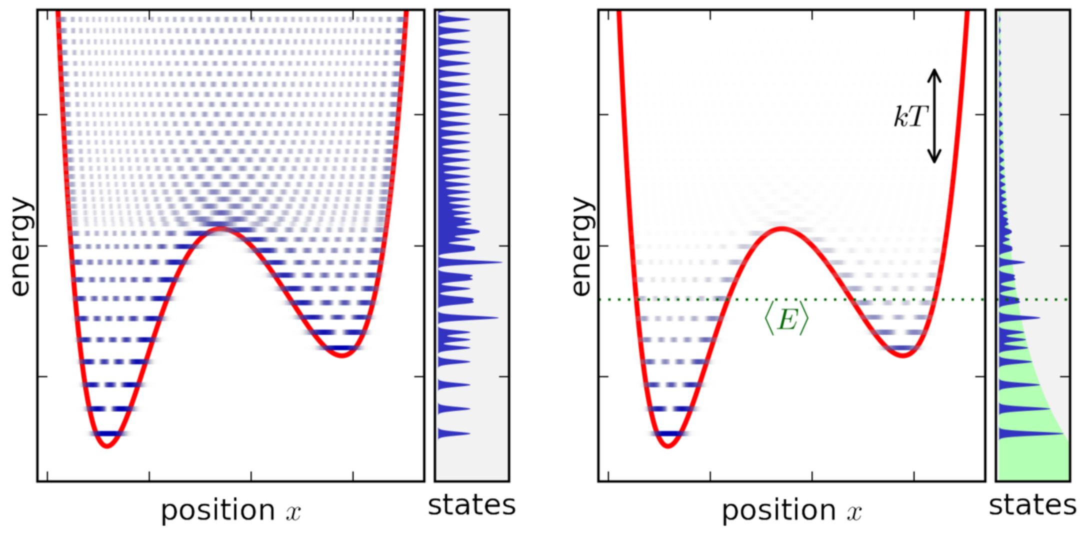

Figure 3.1: Ensemble canonically distributed over energy, for a quantum system consisting of one particle in a potential well: dependency of number of states, temperature and energy of the system [89].

Then probability p_i of the state i is defining as Boltzmann-Gibbs distribution in thermodynamic equilibrium conditions between the mechanical system and environment which is represented as

$$p_i = \frac{1}{Z} \exp\left(-\frac{E_i}{k_B \cdot T}\right) \quad \text{and} \tag{3.1}$$

$$\sum_i p_i = 1, \tag{3.2}$$

where T is absolute temperature, k_B is the Boltzmann constant, E_i is some energy of the whole mechanical system, Z is the *partition* (normalization) function

$$Z = \sum_i \exp\left(-\frac{E_i}{k_B \cdot T}\right). \tag{3.3}$$

Boltzmann probability distribution (3.1) is an exponential distribution which is derived from the *Gibbs canonical distribution* and *canonical ensemble*, for more details see statistical mechanics [84], [49], [20].

The main theoretical facts from statistical physics about energy function [49] which are playing the basis role in the *Energy-Base learning* [55], [53], [68] and will be used in Restricted Boltzmann Machine:

1. state with low energy has more chances to appear than state with high energy;
2. when the temperature is decreasing states will appear more frequently from the small subset of states with low energy, see Figure 3.1. That is when the temperature T is high then particles move «more chaotically», the system has more states and can easily move from state to state. When the temperature T is reduced number of system states is decreasing. In ideal case system will have just one state when the temperature $T = 0$.

3.2 Restricted Boltzmann Machine inference

A Restricted Boltzmann machine (RBM) is a generative stochastic artificial neural network that can learn a probability distribution over its set of inputs. RBM was originally invented under the name Harmonium by Paul Smolensky in 1986 [81]. It became very popular only after Geoffrey Hinton and collaborators developed training algorithm for RBM [18]. It found applications in dimensionality reduction [41], classification [51], collaborative filtering [75], feature learning [21] and topic modeling [74].

So far, in Section 2 we consider neural networks that could learn to predict from an input a particular target or class labels, that we have seen with Feed-forward neural network. Now we are going to consider unsupervised RBM training that would learn something about data based on the training input vector $\boldsymbol{x}$, this approach extracts meaningful features from the data. However, it can be trained in supervised way as well. RBM also allows us a leverage of the availability of the unlabeled data. When we have small amount of labeled training set and we also have a lot of unlabeled samples. This is called a semi-supervised learning problem.

RBM is an undirected bipartite graphical model shown on Figure 3.2. It defines the distribution over the input vector ***x*** (layer of *visible units*), it is going to model the distribution of these training data using layer of *hidden units* ***h***. Notice, for simplicity, that ***x*** and ***h*** are binary random variables, such RBM is called *Bernoulli-Bernoulli*. There are also *Gaussian-Bernoulli* (real valued ***x*** and binary ***h***) and *Gaussian-Gaussian* (real valued ***x*** and real valued ***h***). Later we explain how to generalize to other types of units that might be a real value.

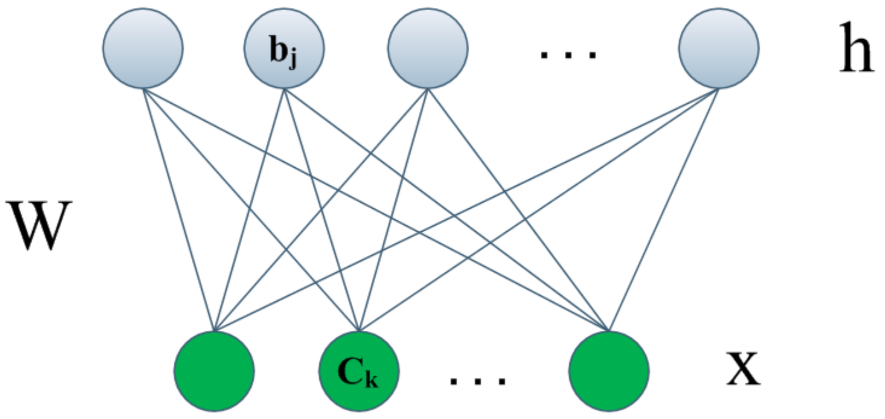

Figure 3.2: Restricted Boltzmann Machine topology.

In order to define the distribution of training set which involves the latent variables which corresponds to hidden units ***h***, let first define the *Energy Function*:

$$E\left(x,h\right) = -h^TWx - c^Tx - b^Th, \tag{3.4}$$

where $h \in \{0,1\}^{N_h\times 1}$ is the vector of hidden units, $x \in \{0,1\}^{N_x\times 1}$ is the vector of visible units, $W \in \mathbb{R}^{N_h\times N_x}$ is the matrix of connection weights, $c \in \mathbb{R}^{N_x\times 1}$ and $b \in \mathbb{R}^{N_h\times 1}$ are the bias vectors.

The probability of the state (x,h) with the Energy Function $E(x,h)$ of the visible and hidden units configuration is defined using Boltzmann-Gibbs distribution (3.1)

$$p\left(x,h\right) = \frac{\exp\left(-E\left(x,h\right)\right)}{Z}, \tag{3.5}$$

where $Z = \sum\limits_{x,h} e^{-E(x,h)}$ is the normalization factor known as the *partition function*. Unfortunately, partition function is intractable for RBM and later we are going to avoid its calculation [93].

Let consider inference of the posterior probability of h given visible input x. The first fact to know is that the full conditional distribution factorizes. It can be written as the product of each individual hidden unit given vector of visible units:

$$p\left(h|x\right) = \prod_j p\left(h_j|x\right). \tag{3.6}$$

We can easily prove this

$$p\left(h|x\right) = \frac{p\left(x,h\right)}{\sum\limits_{\tilde{h}} p\left(x,\tilde{h}\right)} =$$

$$= \frac{\exp\left[h^T W x + c^T x + b^T h\right]}{\sum\limits_{\tilde{h}\in\{0,1\}^{N_h}} \exp\left[\tilde{h}^T W x + c^T x + b^T \tilde{h}\right]} =$$

$$= \frac{\exp\left[\sum\limits_j h_j W_{j,*} x + b_j h_j\right]}{\sum\limits_{\tilde{h}_1} \cdots \sum\limits_{\tilde{h}_{N_h}} \exp\left[\sum\limits_j \tilde{h}_j W_{j,*} x + b_j \tilde{h}_j\right]} =$$

$$= \frac{\prod\limits_j \exp\left[h_j W_{j,*} x + b_j h_j\right]}{\sum\limits_{\tilde{h}_1} \cdots \sum\limits_{\tilde{h}_{N_h}} \prod\limits_j \exp\left[\tilde{h}_j W_{j,*} x + b_j \tilde{h}_j\right]} =$$

$$= \prod_j \frac{\exp\left[h_j W_{j,*} x + b_j h_j\right]}{\sum\limits_{\tilde{h}_j\in\{0,1\}} \exp\left[\tilde{h}_j W_{j,*} x + b_j \tilde{h}_j\right]} =$$

$$= \prod_j \frac{\exp\left[h_j W_{j,*} x + b_j h_j\right]}{1 + \exp\left[b_j + W_{j,*} x\right]} = \prod_j p\left(h_j|x\right).$$

where $W_{j,*}$ denotes the j-th row of matrix W. It means that all the hidden units are conditionally independent given the values of the visible layer. It is obvious because of the topology of the RBM, hidden units have no connections with each other.

Remind that we consider binary hidden and visible random vectors, i.e. Bernoulli-Bernoulli RBM. Then we can derive probability when hidden unit is equal to one given visible vector:

$$p\left(h_j = 1|x\right) = \frac{1}{1 + \exp\left[-\left(b_j + W_{j,*}x\right)\right]} =$$

$$= \sigma_{logistic}\left(b_j + W_{j,*}x\right), \tag{3.7}$$

where $W_{j,*}$ denotes the j-th row of matrix W. For the binary visible neurons x given h we have similar symmetrical form of posterior probability:

$$p\left(x|h\right) = \prod_k p\left(x_k|h\right), \tag{3.8}$$

and similarly probability when visible unit is active

$$p\left(x_k = 1|h\right) = \frac{1}{1 + \exp\left[-\left(c_k + h^T W_{*,k}\right)\right]} =$$

$$= \sigma_{logistic}\left(c_k + h^T W_{*,k}\right), \tag{3.9}$$

where $W_{*,k}$ means the k-th column of the matrix W. These previous results can be easily derived.

Notice that inference for RBM hidden units (3.7) is just a sigmoid of the linear transformation and it is equal to computation of the feed-forward neural network with sigmoid unit (2.1) no matter whether binary or real-valued inputs are used. *This fact allows us to use the weights of an RBM to initialize a feed-forward neural network with sigmoidal hidden units* [93].

3.2.1 Free energy function

Further the concept of *free energy function* will be considered. Let us infer the marginal probability of the input vector x. We can write it down as sum of the probability of observing the hidden layer with visible units through the all binary hidden vectors, i.e. we get marginal probability distribution summing over all values of h

$$p\left(x\right)=\sum_{h\in\{0,1\}^{N_h}}p\left(x,h\right)=\sum_{h}\frac{\exp\left[-E\left(x,h\right)\right]}{Z}=$$

$$=\frac{\exp\left[c^Tx+\sum_{j=1}^{N_h}\log\left[1+\exp\left(b_j+W_{j,*}x\right)\right]\right]}{Z}=$$

$$=\frac{\exp\left(-F\left(x\right)\right)}{Z},\tag{3.10}$$

where $W_{j,*}$ denotes the j-th row of matrix W, $F(x)$ is the *free energy function*

$$F\left(x\right)=-\log\left[\sum_{h}e^{-E(x,h)}\right].\tag{3.11}$$

Equation (3.10) can be proved as:

$$p\left(x\right)=\frac{\sum_{h\in\{0,1\}^{N_h}}\exp\left[h^TWx+c^Tx+b^Th\right]}{Z}=$$

$$=\frac{\exp\left[c^Tx\right]\sum_{h_1}\cdots\sum_{h_{N_h}}\exp\left[\sum_{j}h_jW_{j,*}x+b_jh_j\right]}{Z}=$$

$$=\frac{\exp\left[c^Tx\right]\left(\sum_{h_1}\exp\left[h_1W_{1,*}x+b_1h_1\right]\right)\dots\left(\sum_{h_{N_h}}\exp\left[h_{N_h}W_{N_h,*}x+b_{N_h}h_{N_h}\right]\right)}{Z}=$$

$$=\frac{\exp\left[c^Tx\right]\left(1+\exp\left[W_{1,*}x+b_1\right]\right)\dots\left(1+\exp\left[W_{N_h,*}x+b_{N_h}\right]\right)}{Z}=$$

$$=\frac{\exp\left(c^Tx+\sum_{j=1}^{N_h}\log\left[1+\exp\left(W_{j,*}x+b_j\right)\right]\right)}{Z}=\frac{\exp\left(-F\left(x\right)\right)}{Z}.\tag{3.12}$$

So, in order to maximize the probability of the input training x in (3.12) we need to find such rows of weight matrix $W_{j,*}$ and bias b_j that will well align together with that x, i.e. represent meaningful features.

3.3 Contrastive Divergence

After we defined all needed terms and notations for restricted Boltzmann machine, further we consider its training algorithm known as *contrastive divergence* [39]. In order to train the RBM parameters we minimize the negative log-likelihood loss function (NLL)

$$J_{NLL}\left(W,b,c;x\right)=\frac{1}{T}\sum_{t}-\log p\left(x^{(t)}\right), \tag{3.13}$$

where $x^{(t)}$ is the t-th sample from training set. For this purpose the stochastic gradient descent is used. For the stochastic gradient descent the general form of derivative of the loss function is derived in [19]

$$\nabla_\theta J_{NLL}\left(W,b,c;x^{(t)}\right)=\frac{\partial-\log p\left(x^{(t)}\right)}{\partial\theta}=$$

$$=E_h\left[\frac{\partial E\left(x^{(t)},h\right)}{\partial\theta}\middle|x^{(t)}\right]-E_{x,h}\left[\frac{\partial E\left(x,h\right)}{\partial\theta}\right], \tag{3.14}$$

where θ is some model parameters.

The first term in the partial derivative (3.14) is called *positive phase* and depends on the observation $x^{(t)}$. This is expectation over the hidden values h of the partial derivative of the energy function with respect to the model parameters given observation $x^{(t)}$. The second term in the (3.14) is called *negative phase* depends explicitly only on the model. This is the expectation over x and h of the partial derivative of the energy function.

The issue here is that the negative phase is intractable, the reason is that we have the exponential summation on both x and h. Therefore, the *negative phase* term is going to be approximated by a *point estimate* to perform the stochastic gradient efficiently. In order to approximate the formula (3.14) without heavy explicit computations the contrastive divergence algorithm was developed [40]. The idea of the algorithm consists of the three components.

Firstly, the expectation in the *negative phase* $E_{x,h}$ will be replaced by a point estimate at a single observation $\tilde{x}$. So if we have that point estimate then we can do the expectation over the h and find the value of derivation of the loss function (3.14). It says that we do

Monte-Carlo estimation of the expectation with the single data point.

Secondly, we obtain that $\tilde{x}$ by Gibbs sampling from the model distribution. For RBM, Gibbs sampling is efficient technique, because of its topology. Units in visible layer are conditionally independent with each other and the same in the hidden layer. Then we sample all the values in the layer in parallel given the values of the opposite layer and then just alternate between each layer, see Figure 3.3.

The last idea is that we start our Gibbs sampling by initializing the input layer by observable training samples $x^{(t)}$. In practice we do not do Gibbs sampling for a lot iterations, already two or three iterations gives close enough approximation [39].

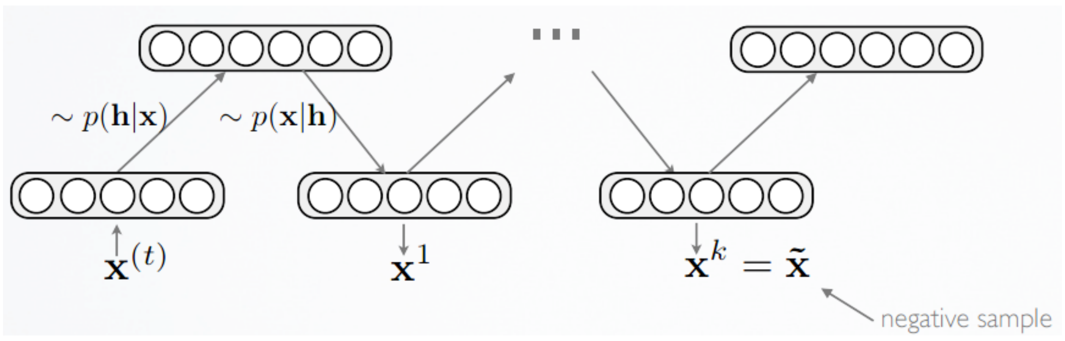
$\sim p(\mathbf{h}|\mathbf{x})$
$\sim p(\mathbf{x}|\mathbf{h})$
...
$\mathbf{x}^{(t)}$
$\mathbf{x}^1$
$\mathbf{x}^k = \tilde{\mathbf{x}}$
negative sample

Figure 3.3: Contrastive divergence schema [50].

On the Figure 3.3 it is shown that during training we take the observation $x^{(t)}$ and set it as a values for the visible layer. Then we sample all the hidden units values condition on observing the particular training sample, i.e. from the distribution $p(h|x^{(t)})$. Notice that all hidden units are conditionally independent and has a Bernoulli distribution, so for each neuron we can compute $p(h_j = 1|x^{(t)})$ by equation (3.7). To obtain a sample from that distribution we can sample using uniform distribution $U[0,1]$ and check the rule of sampling:

$$p(h_j = 1|x^{(t)}) > U[0,1], \tag{3.15}$$

i.e. we have identity function if that sampled value is smaller then the probability value then the value of hidden unit h_j is set to 1, otherwise 0.

So, we sampled each hidden units conditioned on the observable values. Then we are going to reconstruct the visible layer by sampling from the distribution $p(x|h)$ given values of the hidden layer which we got on the previous step. Therefore, we get x^1 and so on and so forth. We continue to iterate Gibbs sampling for k steps. After k steps the *negative sample* is approximated as $\tilde{x} = x^k$, which will be used to approximate the *negative phase* of the loss function gradient.

Further we will explain the visual intuition of the contrastive divergence. So, we get training example $x^{(t)}$ and in the *positive phase* from the gradient (3.14) the expectation E_h was estimated just by Gibbs sampling $h \sim p(h|x^{(t)})$, and we called the result of sampling as $\tilde{h}^{(t)}$

$$E_h\left[\left.\frac{\partial E\left(x^{(t)},h\right)}{\partial\theta}\right|x^{(t)}\right] \approx \frac{\partial E\left(x^{(t)},\tilde{h}^{(t)}\right)}{\partial\theta}. \tag{3.16}$$

Similarly in the *negative phase* from the gradient (3.14) expectation $E_{x,h}$ is approximated at $\tilde{x}$ and $\tilde{h}$ (after k steps of Gibbs sampling)

$$E_{x,h}\left[\frac{\partial E\left(x,h\right)}{\partial\theta}\right] \approx \frac{\partial E\left(\tilde{x},\tilde{h}\right)}{\partial\theta}, \tag{3.17}$$

where $\tilde{h}$ is the result of sampling $\tilde{h} \sim p(h|\tilde{x})$.

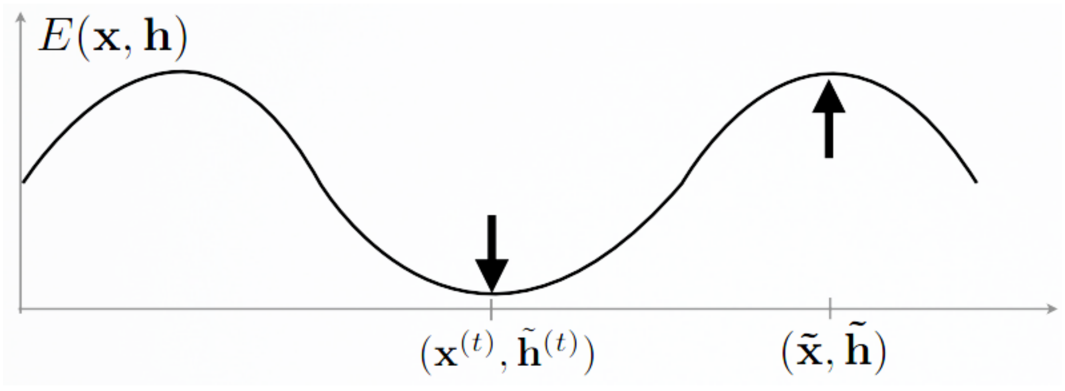
$E(\mathbf{x},\mathbf{h})$
$(\mathbf{x}^{(t)},\tilde{\mathbf{h}}^{(t)})$
$(\tilde{\mathbf{x}},\tilde{\mathbf{h}})$

Figure 3.4: Contrastive divergence energy function [50].

Visually the training process can be presented as Figure 3.4. It says that we should decrease the energy at the training observation $\left(x^{(t)},\tilde{h}^{(t)}\right)$ and increase at the state $\left(\tilde{x},\tilde{h}\right)$. It is because the low energy values corresponds to high probability. This means that we are going to increase the probability of state $\left(x^{(t)},\tilde{h}^{(t)}\right)$ and at the same time decrease at $\left(\tilde{x},\tilde{h}\right)$.

For example, if we have image of digit as the training sample (see Figure 3.5) then we are going to increase probability of observing the particular digit at the model state $\left(x^{(t)},\tilde{h}^{(t)}\right)$, and at the begining the RBM is initialised randomly from the binary uniform distribution,

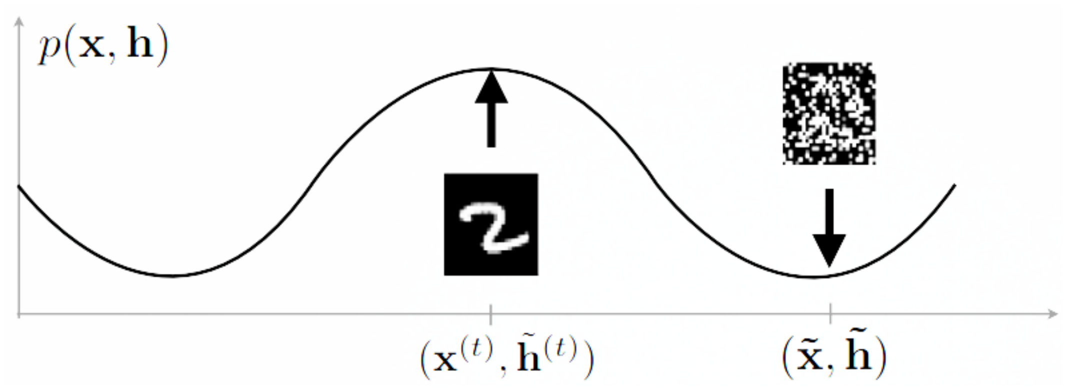
$p(\mathbf{x}, \mathbf{h})$
$(\mathbf{x}^{(t)}, \tilde{\mathbf{h}}^{(t)})$
$(\tilde{\mathbf{x}}, \tilde{\mathbf{h}})$

Figure 3.5: Contrastive divergence probability function [50].

it is really look like noise. As we continue training our model by sampling, the gradient becomes smaller because the sampled value $\tilde{x}$ becomes more similar to train sample $x^{(t)}$.

Intuitively what is the contrastive divergence doing is that it is decreasing the energy for the sampled values that look like training examples and increasing the energy of the nosy samples produced by the model and we keep doing the sampling until the RBM produce the sample $\tilde{x}$ which is similar to the example from the training set $x^{(t)}$. During this sampling our model parameters matrix of weights W and biases b and c are tuning.

Further, lets derive the update rule for RBM model parameters. In order to obtain the derivation of the loss function (3.14) the derivation $\frac{\partial E(x,h)}{\partial \theta}$ for $\theta = w_{jk}$ will obtained as

$$\frac{\partial E\left(x,h\right)}{\partial w_{jk}} = \frac{\partial}{\partial w_{jk}}\left(-\sum_{jk} w_{jk}h_j x_k - \sum_k c_k x_k - \sum_j b_j h_j\right) =$$

$$= -\frac{\partial}{\partial w_{jk}}\sum_{jk} w_{jk}h_j x_k = -h_j x_k, \tag{3.18}$$

and in matrix form we get

$$\nabla_W E\left(x,h\right) = -hx^T. \tag{3.19}$$

If we consider the expectation with respect to h conditioned on any given training sample x and take into account the previous derivation (3.19)

$$E_h\left[\left.\frac{\partial E\left(x,h\right)}{\partial w_{jk}}\right| x\right] = E_h\left[\left.-h_j x_k\right| x\right] = \sum_{h_j\in\{0,1\}} -h_j x_k p\left(\left.h_j\right| x\right) =$$

$$= -x_k p\left(\left.h_j = 1\right| x\right), \tag{3.20}$$

where if we define $h(x)$ as

$$h\left(x\right) \overset{def}{=} \begin{pmatrix} p\left(\left.h_1 = 1\right| x\right) \\ \cdots \\ p\left(\left.h_{N_h} = 1\right| x\right) \end{pmatrix} = \sigma\left(b + Wx\right), \tag{3.21}$$

then (3.20) in matrix form

$$E_h\left[\left.\nabla_W E\left(x,h\right)\right| x\right] = -h\left(x\right) x^T. \tag{3.22}$$

If we put everything together we will get the updating rule for weight matrix [10]. For given training sample $x^{(t)}$ and k-steps Gibbs sampled vector $\tilde{x}$ the learning rule for weight parameters $\theta = W$ becomes

$$W := W - \alpha \cdot \nabla_W\left(-\log p\left(x^{(t)}\right)\right) =$$

where α is a learning rate, using equation (3.14)

$$= W - \alpha\left(E_h\left[\left.\nabla_W E\left(x^{(t)},h\right)\right| x^{(t)}\right] - E_{x,h}\left[\nabla_W E\left(x,h\right)\right]\right) =$$

using positive and negative point estimates (3.16) and (3.17)

$$= W - \alpha\left(E_h\left[\left.\nabla_W E\left(x^{(t)},h\right)\right| x^{(t)}\right] - E_h\left[\left.\nabla_W E\left(\tilde{x},h\right)\right| \tilde{x}\right]\right) =$$

using (3.19) and (3.22)

$$= W + \alpha\left(h\left(x^{(t)}\right) x^{(t)^T} - h\left(\tilde{x}\right)\tilde{x}^T\right). \tag{3.23}$$

Similarly updating rule for biases b and c can be derived, see details in [10], [33].

The general pseudo code for contrastive divergence is presented in Algorithm 2.

Algorithm 2 Contrastive divergence (CD_1) [10]

This is RBM algorithm for Bernoulli-Bernoulli units. It can easily adapted to other types of units.

Input: $x^{(t)}$ – training sample;
α – learning rate;
Output: matrix of weights W and biases b, c;

```
1: repeat
2:     randomly choose $x^{(t)}$;
3:     Generate $\tilde{x}$: Gibbs sampling $k = 1$ steps starting from $x^{(t)}$;
       • compute $p(h|x^{(t)})$ using (3.21);
       • sample $h^{(0)} \in \{0,1\}^{N_h}$ from $p(h|x^{(t)})$;
       • compute $p(x|h^{(0)})$ using (3.9);
       • sample $\tilde{x} = x^{(1)} \in \{0,1\}^{N_x}$ from $p(x|h^{(0)})$;
4:     compute $h(\tilde{x})$ using (3.21);
5:     update parameters:
```

$$W := W + \alpha \left(h^{(0)} x^{(t)^T} - h\left(\tilde{x}\right) \tilde{x}^T \right); \tag{3.24}$$

$$b := b + \alpha \left(h^{(0)} - h\left(\tilde{x}\right) \right); \tag{3.25}$$

$$c := c + \alpha \left(x^{(t)} - \tilde{x} \right); \tag{3.26}$$

```
6: until stopping criteria;
```

Notes on Contrastive Divergence. Usually for contrastive divergence contraction CD_k is used, it means that k iterations of Gibbs sampling was used. In general the bigger k is, the less biased the gradient estimation will be and close to the model expectation. In practice $k = 1$ is enough in such problems as feature extraction or neural networks pre-training [10].

CHAPTER 4

Convolutional Neural Networks

Convolutional Neural Networks (CNN) firstly were applied for computer vision problems. CNN were specifically designed and adapted for image recognition problems [13, 12]. One of the issues in computer vision is that 2D image has very high-dimensional inputs (e.g. 150×150 pixels $= 22500$ inputs for gray scale or 3×22500 if RGB pixels). If "fully connected" network (all the hidden units are connected to all the input units) was used it would be computationally unfeasible to learn features on the entire image. On top of that, we would get a lot of redundant information and parameters, hence, it is easy to overfit [13, 46].

In computer vision there is a problem of dimensionality reduction of image, in order to solve this problem the 2D spatial topology of pixels is exploited (or 3D for video data). Also the invariances to certain distortions (translations, illumination, etc.) is taken into account and should not affect the result of recognition but generalize the input features. CNN found successful application in automatic speech recognition (ASR) as well [2, 3, 73, 72], because of the series of properties such as *local connectivity*, *parameter sharing* and *pooling* [33].

First, let us define a convolution operation with basic definitions and then we will present some properties of CNN which are utilized in ASR.

Discrete convolution of two functions x and w which are defined only on integer moments t can be defined as in [12]

$$s\left[t\right] = \left(x * w\right)\left(t\right) = \sum_{n=1}^{F} x\left[n\right] w\left[t-n\right], \tag{4.1}$$

where in convolutional network terms the first argument (function x) is referred as the *input* (or *input feature map*), the function w as the *kernel* (or *filter function*) and F is the *filter size*. The filter function is an array of learn-able parameters (weights), and it is much smaller than the input signal x. The output s is called *output feature map*. Usually, convolution operation used in CNN does not correspond precisely to the definition of convolution as used in pure mathematics [15].

The key idea for understanding and designing of CNN is that convolutional networks are simple networks that use convolution operation in place of general multiplication [2]. CNN can be represented as a matrix multiplication with special sparse structure (see next section). This matrix is composed of kernel elements w from (4.1), where each row of the matrix is equal to the row above shifted by one (or several) element. This is known as a *Toeplitz matrix* [7]. Thus, any neural network algorithm that works with matrix multiplication and does not depend on specific properties of the matrix structure should work with convolution [12]. That is why we can easily apply same backpropagation algorithm for training CNN, representing it in matrix form first to infer the algorithm.

4.1 Properties

In this section we focus on the three fundamental properties of Convolutional Neural Network, these are local (sparse) connectivity, parameter sharing and pooling (subsampling) hidden units.

Local connectivity. In general case of conventional feed-forward neural network we have fully connected interactions, i.e. each unit of hidden layer is connected with each input unit. Convolutional networks have *sparse* (or local) *interactions*. This is accomplished by making the kernel smaller then the input feature vector. That is the every unit of the higher layer is computed at a particular position of the sliding window and depends upon features of the local region that the window currently looks upon. Thus, we need to store less parameters, it reduces the memory requirements of the model and improves the computation speed [3]. The convolution of the filter (kernel) with the input signal is demonstrated in the Figure 4.1. For every output unit in the convolution feature map the filter is considering only local limited number of the units from the previous layer, e.g. three adjacent units.

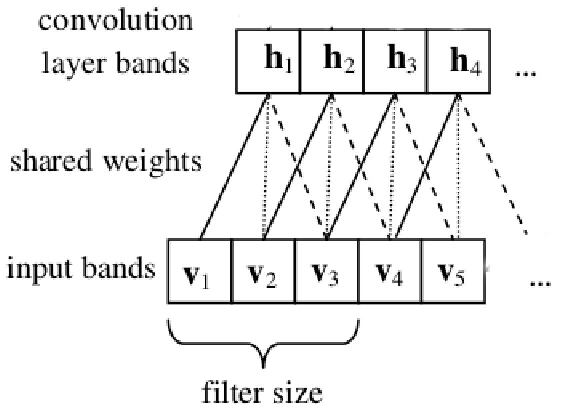

Figure 4.1: Diagram to demonstrate the local connectivity property of convolution layer with filter of size three, connections of the same line style are sharing the same weight. The output layer is the convolution feature map generated by this filter [3].

Weights sharing. *Weights* (or parameters) *sharing* in CNN means that rather than training a separate set of parameters for every location of the kernel, we train only one set. In the Figure 4.1, connections of the same type of lines are restricted to always have the same weight. We can achieve this by initializing all the connections in a group with identical weights and by always averaging the weight updates of a group before applying them at the end of each iteration. Benefits of the weights sharing in ASR are the next: it can improve model robustness and reduce overfitting, because each weight is learned from multiple frequency bands in the input instead of just from one single location [46].

Pooling. *Pooling* or *subsampling* usually is applied to convolution feature maps after convolution operation on input signal. Each map from the convolutional layer is subsampled typically with mean or max pooling over $p \times p$ contiguous regions. That is pooling replaces the local number of units with one summary statistic of nearby outputs. Pooling operation makes the representation becomes *invariant* to small translations of the input, i.e. introduce invariance to local translations and distortions. Another property of pooling is that it reduces the number of hidden units in hidden layers, i.e. reduces dimensionality of the convolution feature maps. Pooling property improves speech recognition performance. It makes CNN more robust to slight formant shifts at a local frequency region due to speaker or speaking style variation [46].

4.2 Network architecture

In Figure 4.2, a CNN consists of three types of layers, these are convolutional layers, pooling layers and fully-connected layers. In a convolution layer, each neuron takes inputs from a small rectangular section of the previous layer, multiplying those local inputs against the weight matrix, or convolution kernel, W. The weight matrix will be replicated across the entire input space to detect a specific kind of local pattern. All neurons in convolution layer which are share the same weights compose a feature map. Convolution layer consists of many feature maps produced by different weight filters to extract multiple kinds of local patterns at every location. The number of feature maps exactly correspond to the number of local weight filters used in convolutional mapping [46].

After convolutional layer the next layer is pooling. The pooling layer takes local region of units from the previous layer and down-sample that region to get a single output signal from that region. Usually it is used max-pooling operation, which takes maximal value from local region. Therefore, this operation reduces the dimension of the feature maps from the convolutional layer (see Figure 4.2). Finally, after series of one or more convolutional-pooling building blocks the fully-connected hidden layers continue the CNN architecture. The output signal from the CNN is produced by the softmax or sigmoid output layer [93]. So far we described the principal architecture of CNN. Further in this section we will consider CNN components in more detail.

Organizing input features to the CNN. In this research we use *log-Mel filter-bank* features (MFSC) [2] extracted from each speech frame, along with their first and second derivatives [2]. The conventional MFCC features are not suitable here because the discrete cosine transformation produce decorrelated basis. Therefore, MFCC may not maintain locality in both axes of frequency and time [3, 2, 46].

There exist several different alternatives for organizing these vectors of filter-banks into input feature maps for the CNN [2, 3]. In this work we consider feature organization for 1-D Convolutional Neural Networks with convolution only along the frequency axis of the filter-bank spectrogram [2]. Most recent works show that shift-invariance in frequency is more important than shift-invariance in time [46]. In Figure 4.3 feature vectors organized as a 1-D input feature maps for the CNN, convolution operation is applied to these maps.

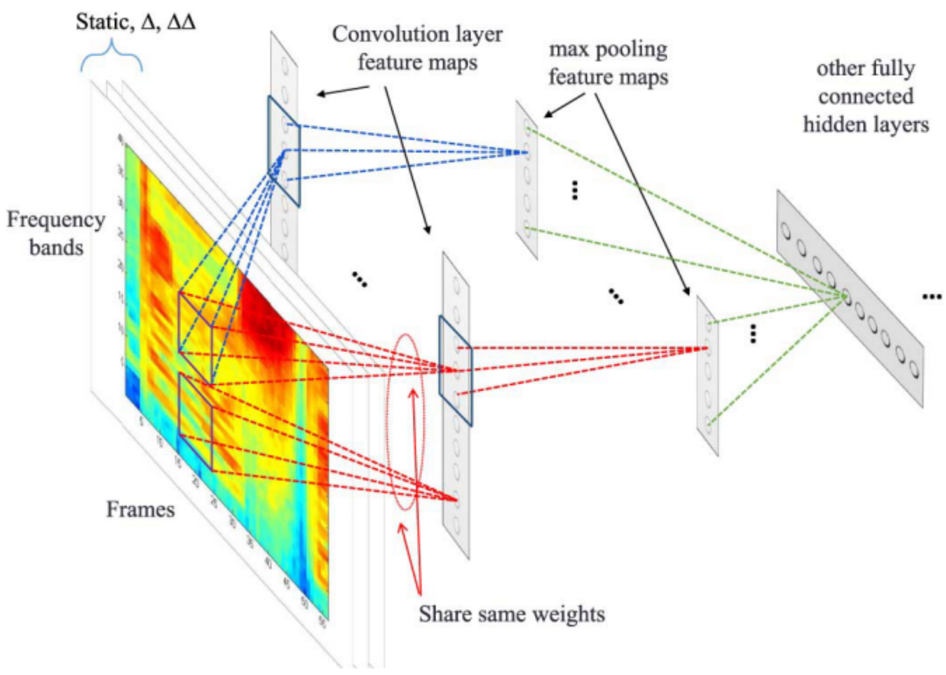

Figure 4.2: Example of the CNN architecture with one convolution, pooling and fully-connected hidden layers [2].

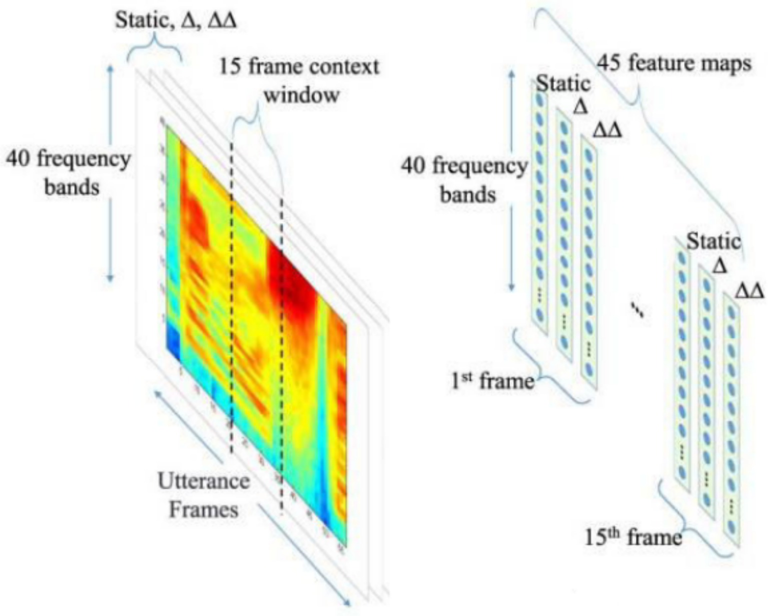

Figure 4.3: Example of CNN input feature organization. It is composed as 1-D feature maps from context window of 15 frames, each having 40 dimensions and first and second derivatives [2].

Convolution and Pooling mapping. If one dimensional input feature maps O_i ($i = \overline{1, I}$, in Figure 4.3 $I = 45$) are used then the convolution operation can be written in matrix form using 1-D convolution mapping $*$, and it produces convolutional feature maps $Q_j (j = \overline{1, J})$, [2]:

$$Q_j = \sigma \left(\sum_{i=1}^{I} O_i * \mathbf{w}_{i,j} \right), \quad j = \overline{1, J}, \tag{4.2}$$

where $\mathbf{w}_{i,j}$ is local weight matrix (kernel), see Figure 4.4. Note that the number of feature maps Q_j in the convolution layer is corresponding to the number of weight matrices $\mathbf{w}_{i,j}$. In practice, we will constrain many of these weight matrices to be identical. In other words, the single feature map Q_j is produced by convolving all input maps O_i with the same kernel $\mathbf{w}_{i,j}$.

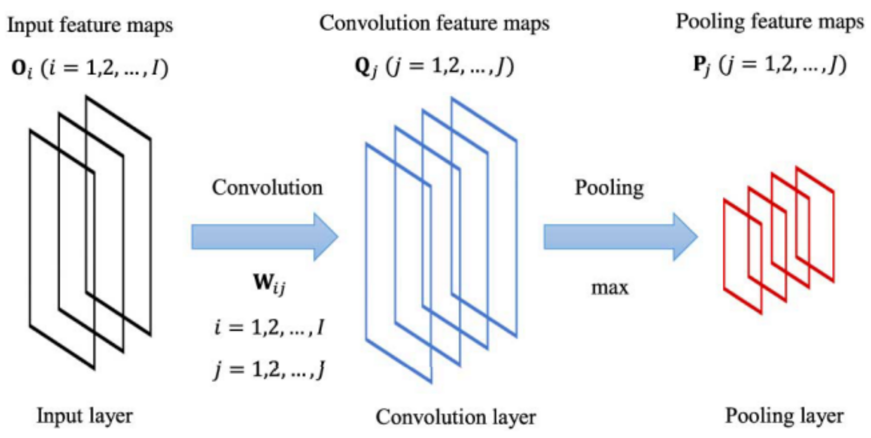

Figure 4.4: An illustration of one CNN «layer» consisting of a pair of a convolutional and pooling layers in succession, where mapping from input layer to a convolutional is based on eq. (4.2) and mapping from a convolution ply to a pooling ply is based on eq. (4.3) [2].

The max-pooling mapping can be written as in [2]

$$p_{j,m} = \max_{n=1}^{G} q_{j,(m-1)\times s+n}, \tag{4.3}$$

where G is the *pooling size*, s is the *shift size* and $p_{j,m}$ is the m-th unit of the j pooling feature map. The pooling function is applied to every convolution map independently and consider local region of units, the size of that region is called *pooling size*.

After pooling operation neural network has the same number of feature maps as the number of feature maps in its convolution layer, but each map is smaller. The purpose of the pooling is to reduce the resolution of feature maps. After a sequence of convolutional-pooling blocks signal comes to usual fully-connected feed-forward neural network. For training the whole Convolutional Neural Network the backpropagation algorithm can be applied [2].

CHAPTER 5

Deep Neural Network Pre-training

5.1 Motivation for deepness

There are several hypothesis that encouraged scientists to consider neural networks to be multilayers and have deep topology. As it was mentioned earlier in Chapter 2 that scientists were inspired by neurophysiology in order to develop artificial neural networks, they went further. It was proved in biology that there are many types of neurons in brain and all of them are not chaotically connected but organize some groups and neural ensembles [35], [16]. These neural ensembles form some levels of abstraction from primitive on the input sensors to high levels when signal spreads further. They utilize this idea in mathematical models of deep neural networks, see Figure 5.1.

The universal approximation theorem (Theorem 1) does not say about number of hidden layers or units. There was the question it is better to train one layer network with many units or deep network with less units. More formal mathematical motivation for deepness of neural networks was proved by Y. Bengio in [10]. He showed that $k + 1$ - layer nets can easily represent what a k - layer net can represent, whereas the converse is not true, i.e. deeper networks have more generalization capacity.

Therefore, scientists were motivated to have deep topologies, but there were no training algorithm for them. Experiments showed that training deep architectures is more difficult than training shallow networks [11, 26]. It was suggested that supervised gradient-based training of deep multi-layer neural networks, starting from random weights initialization, gets stuck in local minima or plateaus [10]. When architecture gets deeper the vanishing

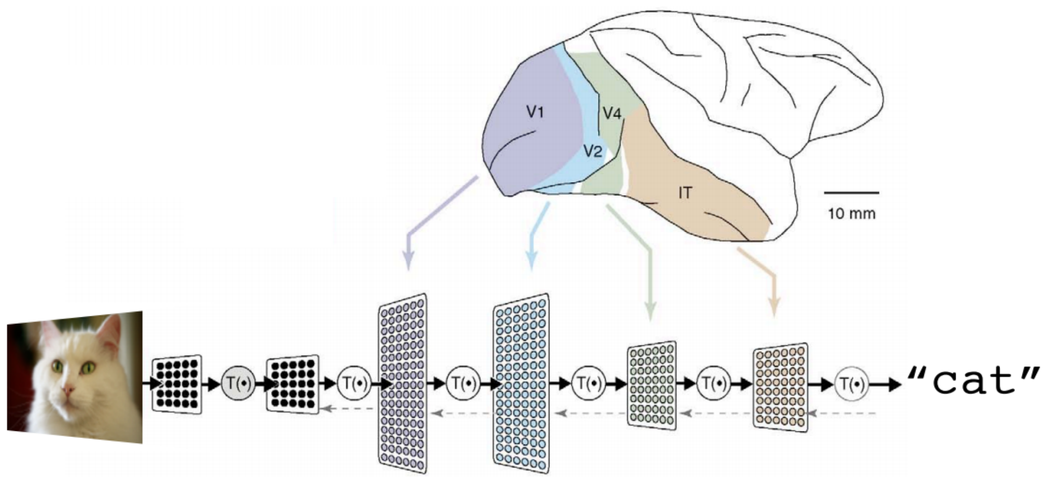

Figure 5.1: Layers of deep neural network as a levels of brain abstractions [23]. According to natural brain model of visual system the next neural layer learns new level of abstractions (e.g. dots $\rightarrow$ dashes $\rightarrow$ surface and lines $\rightarrow$ objects).

gradient problem brings difficulties to obtain solution.

However, it was revealed that much better results could be archived when pre-training each layer one by one with an unsupervised learning algorithm [40] such as the RBM generative model. After having initialized a number of layers, the whole neural network can be fine-tuned with respect to a supervised training approach as usual. The advantage of unsupervised pre-training versus random initialization was demonstrated in [11, 69, 86].

5.2 Deep Belief Network pre-training

In this paragraph we will see how Restricted Boltzmann Machines played important role for whole Deep Learning [40]. *Deep Belief Networks* is the method which lies in the origin of the unsupervised layer-wise pre-training for deep feed-forward networks that we have seen before. DBN is a hybrid generative model that mixes undirected and directed connections between units which constitute the network [40], [37].

On the Figure 5.2 example topology of DBN is presented. It has three hidden layers marked as h and visible x. It has undirected connections between $h^{(3)}$ and $h^{(2)}$ layers and directed between others. In DBN topology, the top two layers will always form Restricted Boltzmann Machine network. In other words in our example the distribution $p\left(h^{(2)}, h^{(3)}\right)$ is defined by RBM with undirected connections.

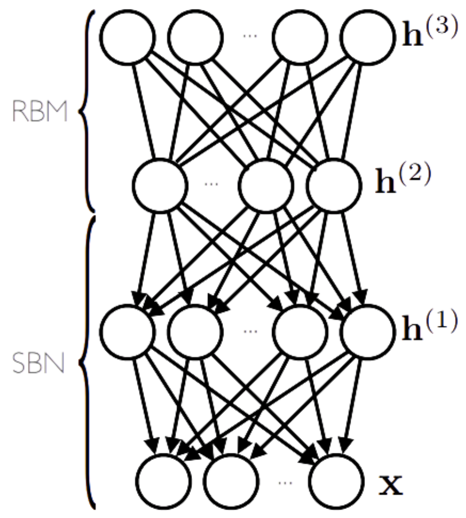

Figure 5.2: Example of Deep Belief Network topology with three hidden layers.

Other layers form a Bayesian network instead with top-down directed interactions. Specifically the conditional distributions of the units in these layers given the layer above is going to take this form

$$p\left(h_j^{(1)} = 1 \middle| h^{(2)}\right) = \sigma\left(b^{(1)} + W^{(2)^T} h^{(2)}\right), \tag{5.1}$$

$$p\left(x_j^{(1)} = 1 \middle| h^{(1)}\right) = \sigma\left(b^{(0)} + W^{(1)^T} h^{(1)}\right). \tag{5.2}$$

So this corresponds to the probabilistic model associated with the logistic regression model. That is the probability of the hidden unit $h_j^{(1)}$ or visible unit $x_j^{(1)}$, which are supposed to be equal to one, is a sigmoid applied to linear transformation of the layer above. When we have units that interact in this way we call such a model *Sigmoid Believe Network* (SBN) [40].

So the Deep Belief Network is a model the top two layers form an RBM while the bottom layers form a SBN and units are not connected with each other in one layer, only neighbor layers are connected. In order to generate data from the DBN (see example in [36]) we would need to do Gibbs sampling between the top two layers in the RBM for the very long time. Once we have converge to an equilibrium distribution and $h^{(2)}$ is sampled from its the actual prior distribution $p\left(h^{(2)}, h^{(3)}\right)$.

Then from $h^{(2)}$ we would directly generate $h^{(1)}$ using stochastic equations (5.1) and from $h^{(1)}$ we would generate directly x using (5.2). That would give us an observation or a sample from the input layer x from a Deep Belief Network. It is a generative process associated with DBN.

Notice that DBN is not a feed-forward network. Sometimes in a literature they say «stacked RBMs are a deep belief network». If we would do that, i.e. just stacking the RBMs and initialize a feed-forward network, we do not call this network as a deep belief network. We would call it as unsupervised RBMs' pre-training for feed-forward network. The DBN is a specific model where the hidden units are stochastic and binaries and the topology is as RBM-SBN, as it was said above.

The probabilistic model of DBN is the next the joint distribution over the input and three hidden layers (for our example of three hidden layers)

$$p\left(x, h^{(1)}, h^{(2)}, h^{(3)}\right) = p\left(h^{(2)}, h^{(3)}\right) p\left(h^{(1)}\middle| h^{(2)}\right) p\left(x\middle| h^{(1)}\right), \tag{5.3}$$

where the prier probability of $h^{(2)}$ and $h^{(3)}$ has form

$$p\left(h^{(2)}, h^{(3)}\right) = \exp\left(h^{(2)^T} W^{(3)} h^{(3)} + b^{(2)^T} h^{(2)} + b^{(3)^T} h^{(3)}\right) \Big/ Z, \tag{5.4}$$

which is exactly an RBM probability function (3.5).

The probability of $h^{(1)}$ given $h^{(2)}$ is the part of the sigmoid belief network

$$p\left(h^{(1)}\middle| h^{(2)}\right) = \prod_j p\left(h_j^{(1)}\middle| h^{(2)}\right). \tag{5.5}$$

Finally, we get x sampled from layer $h^{(1)}$

$$p\left(x\middle| h^{(1)}\right) = \prod_i p\left(x_i\middle| h^{(1)}\right). \tag{5.6}$$

The main fact here is that training the DBN is a hard computational problem [38]. It turns out that a good initialization plays a crucial role on the quality of results. This is in fact how ***greedy layer-wise pre-training*** *[40] approach was developed as a way of initialization better parameters for deep belief network. After that it was noticed that we can use same initialization to improve training of the feed-forward neural networks.* So, this is how the idea of stacking of RBMs for pre-training came from that problem described above.

The idea for the initialization procedure is that in order to train three hidden layer DBN we will start from one hidden layer DBN. One hidden layer DBN is just an RBM part of DBN (see Figure 5.3), because we take top two layers and there are no sigmoid belief layers.

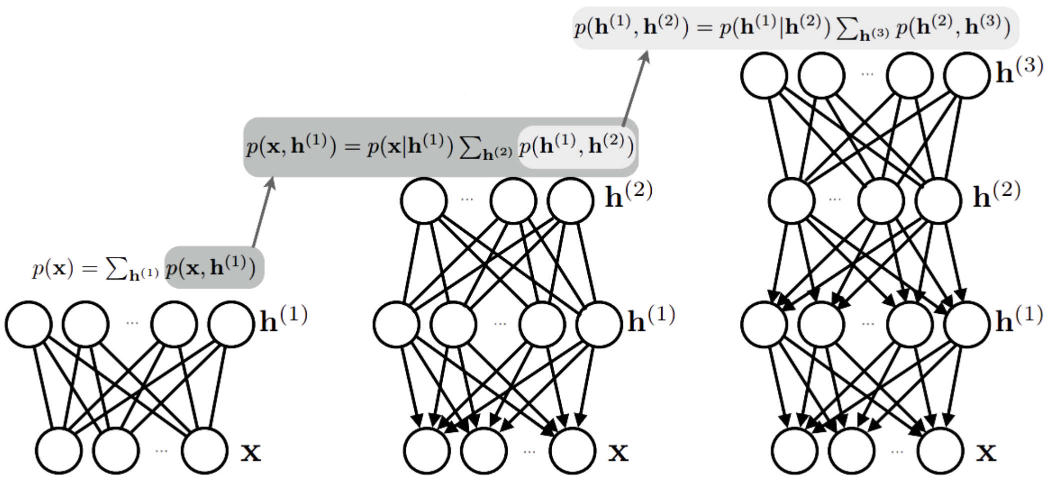
$p(\mathbf{h}^{(1)}, \mathbf{h}^{(2)}) = p(\mathbf{h}^{(1)}|\mathbf{h}^{(2)}) \sum_{\mathbf{h}^{(3)}} p(\mathbf{h}^{(2)}, \mathbf{h}^{(3)})$
$p(\mathbf{x}, \mathbf{h}^{(1)}) = p(\mathbf{x}|\mathbf{h}^{(1)}) \sum_{\mathbf{h}^{(2)}} p(\mathbf{h}^{(1)}, \mathbf{h}^{(2)})$
$p(\mathbf{x}) = \sum_{\mathbf{h}^{(1)}} p(\mathbf{x}, \mathbf{h}^{(1)})$
$\mathbf{h}^{(3)}$
$\mathbf{h}^{(2)}$
$\mathbf{h}^{(1)}$
$\mathbf{x}$

Figure 5.3: Pre-training procedure of Deep Belief Network: starts from top RBM (left figure), then add one by one sigmoid belief layers (central and right images) [50].

After training one hidden layer DBN we use its weights for initialization of sigmoid part of two hidden layer DBN (Figure 5.3, central image). In two hidden layer DBN we train again RBM part only with fixed weights for directed connections. The same idea is applied for three hidden layers DBN, initialize and fix low part and train only top two layer RBM. After that pre-training procedure we are doing fine-tuning.

The formal idea is that when we train one hidden layer DBN (RBM) we have a model

$$p\left(x\right) = \sum_{h^{(1)}} p\left(x, h^{(1)}\right), \tag{5.7}$$

which is a marginalization of the hidden layer, which is defined by an RBM.

The part $p(x, h^{(1)})$ we can represent as

$$p\left(x, h^{(1)}\right) = p\left(x \middle| h^{(1)}\right) p(h^{(1)}) = p\left(x \middle| h^{(1)}\right) \sum_{h^{(2)}} p\left(h^{(1)}, h^{(2)}\right), \tag{5.8}$$

when we are passing from one hidden layer to two hidden layers we fix parameters of the $p\left(x \middle| h^{(1)}\right)$ part and train the prier part $p(h^{(1)})$. For $p(h^{(1)})$ we use new RBM which represented as a probability marginalized over $h^{(2)}$.

Then we repeat this procedure for three hidden layers DBN and represent $p\left(h^{(1)}, h^{(2)}\right)$ as

$$p\left(h^{(1)}, h^{(2)}\right) = p\left(h^{(1)} \middle| h^{(2)}\right) p\left(h^{(2)}\right) = p\left(h^{(1)} \middle| h^{(2)}\right) \sum_{h^{(3)}} p\left(h^{(2)}, h^{(3)}\right). \tag{5.9}$$

This is basic idea behind stacking of RBMs in the context of the Deep Belief Networks. In general, procedure of RBMs stacking can be repeated as many time as needed. It produces many layers of non-linear feature detectors that represent progressively more complex statistical structure in the data. That is it was noticed that RBMs layer sequence describes different abstraction levels from primitive to more structured.

5.3 Fine-tunning

Stacking of RBMs (or greedy layer-wise) pre-training gives just good first estimation (starting point) for further fine-tunning. For fine-tunning after pre-training they usually use the *Up-Down algorithm* for generative models [40] (as Deep Belief Networks) or backpropagation for discriminative training.

Notice: *unfortunately, a deep neural network that is pre-trained generatively as a Deep Belief Network, using stack of RBMs, is often still called a Deep Belief Network in the literature, for clarity see [42, 24]. Technically, it is just the same pre-training approach which is applied for initializing weights of feed-forward network and there is nothing else general with DBN. For clarity they call such a pre-trained networks as DBN-DNN [42].*

In this work we are applying discriminative backpropagation fine-tunning. Thus after pre-training a stack of RBMs, we «forget about the whole probabilistic framework» and use the generative weights as initialization for deterministic feed-forward multilayer perceptron (MLP) [42]. On the Figure 5.4 you can see that connections of multilayer perceptron has reversed direction and on top of that we add final softmax layer and train the whole DNN discriminatively. In this work, instead of softmax layer we will use sigmoid layer and mean square error rate loss function.

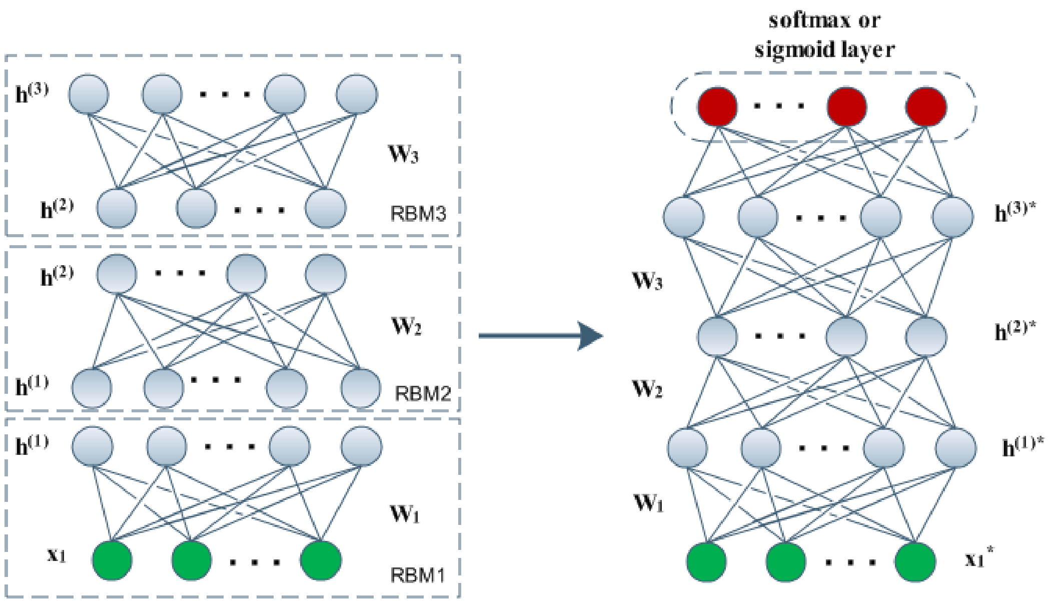

Figure 5.4: Three stacked RBMs on the left figure are used as initialization for feed-forward neural network (or so called DBN-DNN) with three hidden layers. As output layer it could be *softmax* or layer with sigmoid units that output signals one per each attribute label. The DBN-DNN is then discriminatively fine-tuned by backpropagation to predict the attribute label.

CHAPTER 6

Application Neural Networks for Attribute Detection

Speech attributes in natural speech are composed of overlapping several sound events. It means that several attributes may occur at the same time [56, 59, 80]. The goal of this work is to train system which is able to detect every attribute event occuring at any instance of the speech recordings. In this chapter we present frame-based data-driven techniques for speech attributes detection.

The system is implemented using two independent deep neural networks. One of the DNN is for modeling Manner attributes and other is for Place attribute detectors. Moreover for place and manner attributes we investigate two types of deep neural networks, these are DBN-DNN and CNN. We tried to optimize these for the corpora and task by varying number of hidden units and hidden layers and define the best topology.

6.1 System Overview

The problem of the attribute extraction from the speech can be treated as a *multi-label detection* [65, 94]. Here *multi-label* task means that each attribute example can be associated with multiple labels (classes). Therefore, if the size of the label set is N, multi-label detector can associate an example with 2^N different label vectors in general case. The *Detection* task means that we measure probability (or score) that observation belongs to the attribute class.

This task is formally described as the *automatic speech attribute transcription* (ASAT) framework [56]. It is bottom-up detection-based framework, where speech attributes are extracted using data-driven modeling techniques. The goal of each detector is to analyze a speech segment and produce a confidence score or posterior probability that pertains to some acoustic-phonetic attribute. Attributes should be stochastic in nature. Each attribute detector should output probabilities of target class i, non-target and noise model, given a speech frame f: $p\left(H_{target}^{(i)}\middle| f\right)$, $p\left(H_{anti}^{(i)}\middle| f\right)$ and $p\left(H_{noise}^{(i)}\middle| f\right)$. All these probabilities sum up to one, see Figure 6.1.

On this earlier front-end stage of the system we do not need hard decisions from the attribute detectors because of two reasons. First reason, these detectors' outputs will form a new feature vector x by concatenating each of these posterior probabilities from each target classes (7 for manners or 11 for places)[56]. These posterior vectors may be utilized then as a high level features in other components of the system. The second reason, it shifts the responsibility for making decisions on other components which may effectively adjust the risk parameters and introduce additional information for decision making [32].

The first naive idea to solve a multi-label detection problem could be to decompose it into multiple single-label multi-class detection problems, i.e. train detectors to associate each learning example with one of the labels [94]. A network can be trained for each possible class and the results can be combined to get multi-label detection results. However, this method ignores the correlation between the classes and therefore has weak expressive power [94].

In the previous works [56, 79, 80] for speech attribute extraction it was proposed a possible implementation of the ASAT framework, see Figure 6.1. It consists of two main blocks: 1) a bank of *attribute detectors* that can produce detection result in terms of confidence score; and 2) an *evidence merger* that combines low-level events into high-level evidence, such as phone posteriors. Then *append module* stacks together the outputs delivered by the detectors and generate a supervector of attribute detection scores. Every attribute detector was trained using shallow artificial neural networks (ANNs) with cross-entropy cost function and soft-max output layer, hence, simulate the posterior probabilities given the speech frame.

Recently in paper [32] it was proposed promising idea of using cutting edge Deep Neural Network (DNN pre-trained with stack of RBMs) for attribute detectors modeling. All attribute detectors are trained using single DNN and output posterior probability vector after softmax layer, this vector represents all probabilities to be assigned to attribute classes. This model is limited because it outputs posterior probability not per each attribute detector independently for three hypothesis (*target*, *non-target* and *noise*), but it assigns the maximal probability for one class against others, i.e. it represents single-label detector. However, even

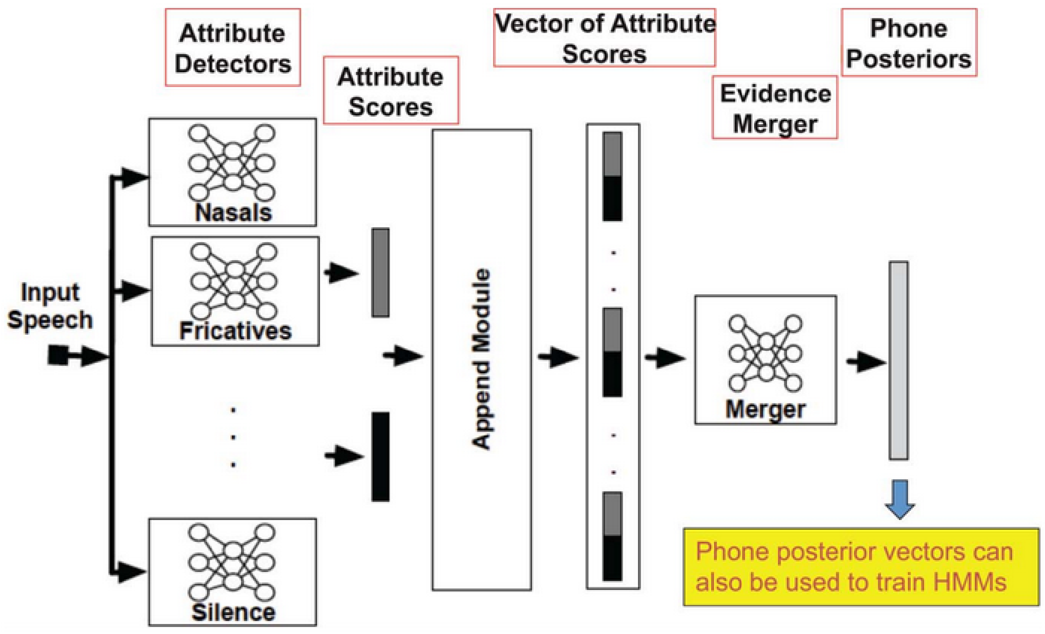

Figure 6.1: Previous attribute detectors' system architecture described in [56]. Every attribute implemented as an artificial neural networks, the outputs are posterior probabilities of a target class i, non-target and noise model, given a speech frame f: $p\left(H_{target}^{(i)}\middle| f\right)$, $p\left(H_{anti}^{(i)}\middle| f\right)$ and $p\left(H_{noise}^{(i)}\middle| f\right)$. All these probabilities sum up to one.

such a limited model has improved results in Foreign Accent Recognition problem [32].

In this research we represent extended idea of the previous work. Here we also use single DNN which model all attribute detectors and produce detection result in terms of a confidence score. We archive that replacing Cross-entropy cost function with Mean Square Error function (MSE), the output soft-max layer is replaced with sigmoid layer. As a result in our proposed system the output scores are not probabilities, but some «posterior» scores which measure the appearance of each attribute independently: $s(Nasals|O(t))$, $s(Fricatives|O(t))$, e.t.c. These scores are in range $[0, 1]$ and produced by the sigmoid units in the output layer of neural network.

In training phase input vector for the DNNs is the concatenated context of speech frames, see Section 6.3. The target output label vector is a binary vector which determined by the manual annotation from OGI dataset (see Section 7.1), its dimension is equal to the number of attribute classes (Manner or Place attributes). If an attribute is annotated as present in data transcription then the corresponding attribute class is marked with 1 in the target output vector, otherwise it is marked with 0. During training the output sigmoid units tried to fit the target label vector using MSE cost function. In testing phase the data is forwarded trough the DNN and produce the confidence scores on the output layer. Thus multi-label detection was solved. These raw output sigmoid scores are directly utilized further in other blocks of the system, however these could be *calibrated* as discussed in [17].

6.2 Speech Feature Extraction

It is conventional in pattern recognition that before training any speech model we need to make a signal preprocessing, extract mostly representative features and reduce the dimensionality to increase computational performance [14]. Such a features are usually represented in time-frequency space.

Here for Neural Networks we extract speech feature vectors of mean-normalized log-filter banks: their static, first and second order derivatives [2], [32]. For extracting log-filter banks it is needed to accomplish usual chain of signal processing. The feature vector was extracted from 25ms sliding window with 10ms shifting using Hamming windowing. After that we apply discrete Fourier transformation on every frame and, finally, logarithm of mel-scale filter bank is applied to power spectrum. Typically, filter banks of 15 to 45 filters are applied to cover the whole frequency range. For DBN-DNN 15 filters were applied, but for CNN 40 filter banks were extracted.

Often in recent literature about DNNs [2, 73, 46] authors directly use log mel-frequency spectral coefficients (filter banks) without a decorrelating discrete cosine transformation (DCTs), it produces an artifacts on the decorrelated mel-frequency cepstral coefficients (MFCC) [2]. Also as it was noticed in Section 4.2, filter bank features after DCT projection may not maintain locality nor along the frequency neither time axis.

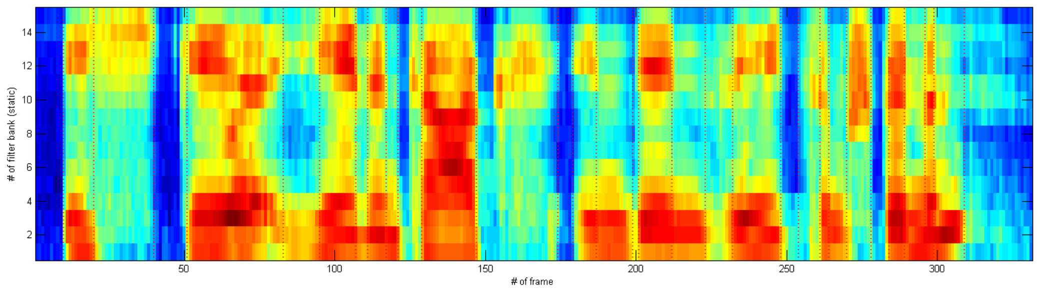

Figure 6.2: Spectrogram of log-filter bank features (15 filters are applied).

6.3 System Settings

We investigate two types of neural networks to solve the problem of attribute detection. The first Deep Network is simple Feed-Forward neural network using Restricted Boltzmann Machine pre-training (context-dependent DBN-DNN, see Chapter 3), the second is Convolutional Neural Network. All experiments are conducted under the context-dependent DNN to extract attribute scores per speech frame

6.3.1 DBN-DNN topology

The input feature vector for DBN-DNN is a 45-dimension mean-normalized log-filter bank features with up to second-order derivatives and a context window of 11 frames, forming an input vector of 495-dimension (45×11). The number of output classes are equal to 7 for manner, and 11 for place. Indeed, the «other» output class is added to both DNN to handle possible unlabelled frames. DNN topologies with 512 and 1024 number of units were studied, number of hidden layers is varying from 1 up to 10 (in total 20 DBN-DNN topologies).

All DBN-DNN topologies are initialized with the stacked Restricted Boltzmann machines using layer by layer generative pre-training, as it was described in Section 5.2. The pre-training algorithm is Contrastive Divergence with 1-step of Markov Chain Monte Carlo sampling (CD-1). The first RBM has Gaussian-Bernoulli units and trained with initial learning rate of 0.01. The following RBMs have Bernoulli-Bernoulli units and a learning rate of 0.4.

After pre-training the weights and stacking all the layers, the final output Sigmoid layer was concatenated with the DNN (see Figure 6.3). The number of output units corresponds to the number of classes (manner or place), these are producing the attribute output scores. The fine-tunning for final weights training is done by mini-batch Stochastic Gradient Decent with learning rate of 0.0008. Mini-batch size is equal to 128 observations. The Mean Square Error objective function was optimized during fine-tunning. In the DNN all Sigmoid hidden units were used. Notice, all settings and parameters are conventional in speech community [42]. During training we did not use momentum or regularization, all training parameter were tracked using RBM guideline by G. Hinton [43].

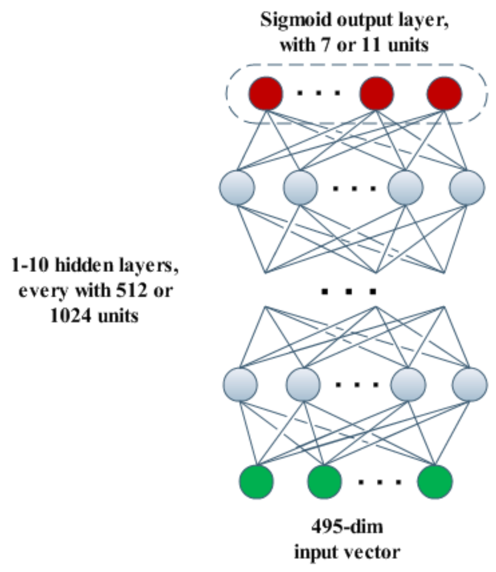
Sigmoid output layer, with 7 or 11 units
1-10 hidden layers, every with 512 or 1024 units
495-dim input vector

Figure 6.3: DBN-DNN topology settings.

6.3.2 Convolutional Neural Networks topology

As shown in Figure 6.4, a 1-D CNN topology, which was trained to detect manner or place attributes, takes input feature maps. These feature maps are organized (as in Figure 4.3) from 40-dimensional log-Mel filter bank features and their first and second-order derivatives, context window is size of 11 frames. In total $3 \times 11 = 33$ input feature maps to which we apply 1-D convolution mapping along the frequency axis. The CNN consists of convolutional layer and max-pooling layer, then from 1 up to 10 fully-connected hidden layers each of them has 512 or 1024 sigmoid units.

Similar to the DBN-DNN settings in case of the CNN we optimize Mean Square Error cost function. Output layer has sigmoid units and produces sigmoid output «posterior» scores for every attribute (7 for manner or 11 for place) per each speech frame.

Convolutional layer in the CNN has 128 feature maps, each of which has size of 33 frequency bands, i.e. these are produced by convolving each input feature map with the filter size of 8 $(1 + (40 - 8) = 33)$. After that max-pooling layer outputs the maximum values over a non-overlapping window covering the outputs of every three frequency bands in each feature map (i.e. pooling size is 3), down-sampling the overall convolutional layer output to three times smaller. Then the output of the max-pooling layer are fed to the fully-connected feed-forward part of the CNN. This CNN architecture follows conventional configurations used in the speech community [73, 46].

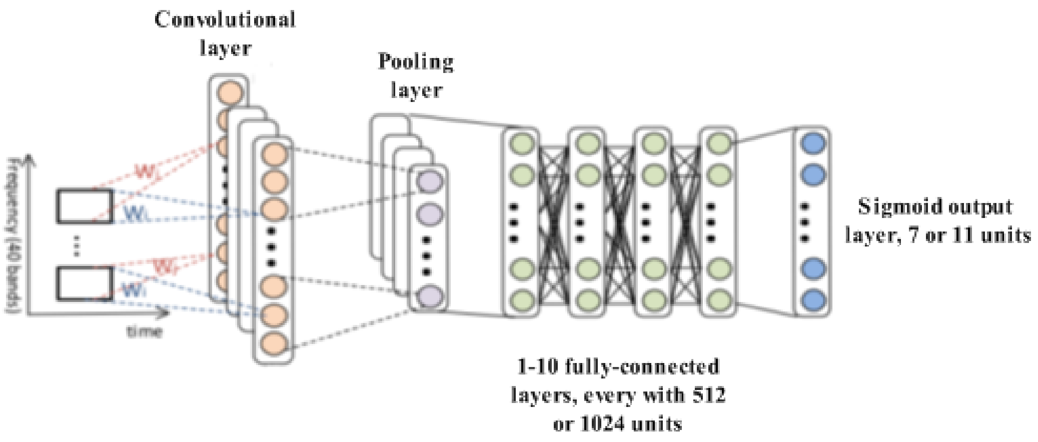
Convolutional layer
Pooling layer
Frequency (40 bands)
time
Sigmoid output layer, 7 or 11 units
1-10 fully-connected layers, every with 512 or 1024 units

Figure 6.4: Convolutional Neural Network topology settings [46].

CHAPTER 7

Experiments and Results

7.1 Dataset

In all experiments the «stories» part of the OGI Multi-language telephone speech corpus [64] was used to train the attribute detectors. This corpus has phoneme transcriptions (with its start and end time in the recordings) for six languages: English, German, Hindi, Japanese, Mandarin, and Spanish. Data from each language were pooled together to obtain around 6 hours of training, 2.5 hours of test and 0.5 hours of cross validation (cv) datasets. Sample rate is 8kHz.

In this work it was used 7 *manner* of articulation classes: **fricative**, **glide**, **nasal**, **silence**, **stop**, **voiced**, **vowel**; and 10 *place* of articulation classes: **coronal**, **dental**, **glottal**, **high**, **labial**, **low**, **mid**, **palatal**, **silence**, and **velar** [80]. Additional class of «other» was added in manner and place, representing any noise or unknown sound events.

Speech attributes can be obtained for a particular language and shared across many different languages, and they can thereby be used to derive a universal set of speech units. Furthermore, data sharing across languages at the attribute level is naturally facilitated by the nature of these classes as shown in [77].

In [78], the authors have demonstrated that manner and place of articulation attributes can compactly characterise any spoken language along the same lines as in the *automatic speech attribute transcription* (ASAT) paradigm for ASR [56]. Furthermore, it was shown that off-the-shelf data-driven attribute detectors built to address automatic language iden-

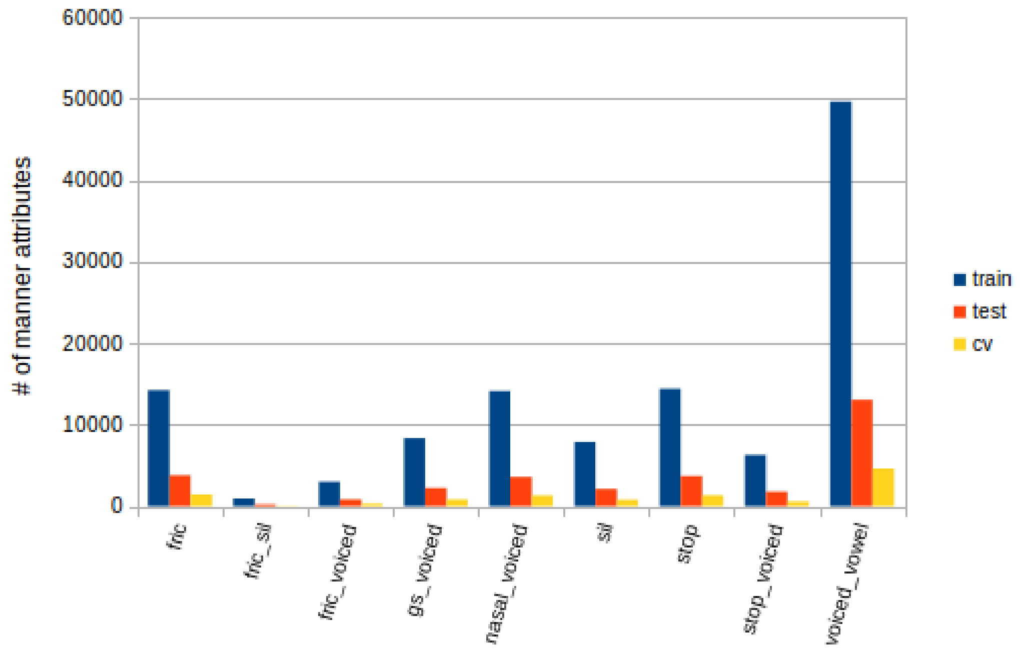

Figure 7.1: Distribution manner of articulation observations in training/test/cv data sets.

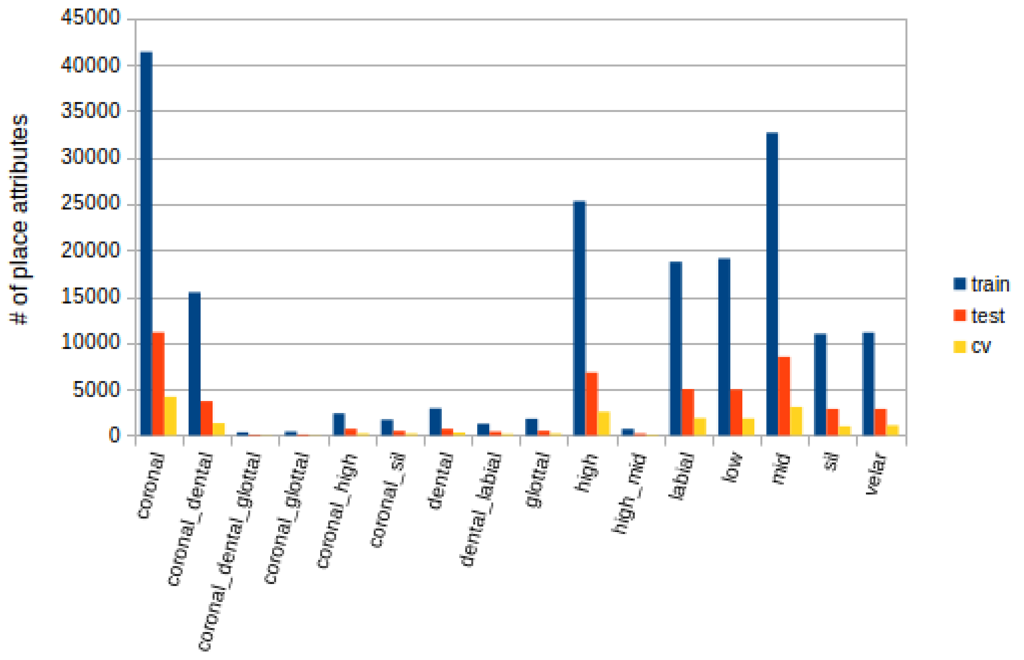

Figure 7.2: Distribution place of articulation observations in training/test/cv data sets.

tification tasks [80] can be exploited without either acoustic adaptation or re-training for characterising speaker accents never observed before [8].

As it was mentioned above the OGI corpus has phoneme transcriptions. In order to train attribute detectors the manner or place transcription were needed, these were obtained from the phoneme transcriptions. We mapped phoneme transcription into corresponding manner or place attributes transcription using mapping tables (Appendix A and B) across all of the languages.

Whenever one phoneme belongs to several attribute classes at the same time we get multiple attribute labels, which names are splitted with underscore (e.g. «fric_voiced»). In other words, it means that these attributes are occurring simultaneously in the speech, and in training target label vector these will be marked with 1 (e.g. for manner of articulation «fric_voiced» will be $[10000010]$ target vector). In testing phase, thanks to sigmoid output layer in neural networks, we can get individual scores in range of (0, 1) which may assign any input observation to multiple attribute classes, as it was discussed in Section 6.1.

Corresponding statistics of the OGI dataset are shown on Figure 7.1 and 7.2. It represents distribution of manner and place observations. Single-label as well as multi-label observations are shown.

7.2 Performance measure

Visual inspection of the *detection error tradeoff* (DET) curves [60] and *equal error rate* (EER) are commonly used evaluation tools for assessing the performance of the models. DET graph shows the tradeoff between two error types: missed detections and false alarm for different values of the threshold, using standard normal deviate axis scale. When there is a tradeoff of error types, a single performance number is inadequate to represent the capabilities of a system. Such a system has many operating points, and is best represented by a performance curve [60]. The Equal Error Rate (EER) measure is used to summarize the performance of a system, defined as the point along the DET curve where the missed detections and false alarm are equal. This may be of use in applications where the cost of each type of error is equal. The lower the number of EER is, the better the system performs.

7.2.1 DET curves

In Figure 7.3, as an example, the DET curves for fricative and voiced manner detectors are presented. One curve on the plot representing detector performance with certain DNN topology, in total 40 different DNN topologies were investigated. The closer curve to the origin the better performance of the corresponding system. On both images it is noticeable that CNN topologies outperform DBN-DNNs. The property of the DET curve is that if resulting curve is close to straight line, then this provides a visual confirmation that the likelihood distributions (for targets and non-targets) from the system are normal. The resulting DET curves for fricative detector are approximately straight lines, whereas the voiced detector curves have the shapes close to convex hyperbolic function and the closest point to the origin is around (8,8).

In Figure 7.4 the velar place detector performance across different models is shown. Here the resulting curves of DBNs and CNNs topologies are densely lying. But still it can be recognized that some CNN curves are closer to the origin, thus outperform DBNs on the all critical operating region. All of the place detectors DET plots have approximately straight performance curves.

7.2.2 Average Equal Error Rate

Average Equal Error Rate (AvgEER) is calculated across all manner and place articulatory detectors and for every particular neural networks model. The average error rate for manners is depicted in Figure 7.5 and depends on the number of hidden layers and number of units. The striking feature to note on the plot is that the CNN models detect attributes better then DBN neural networks, on the whole variety number of hidden layers. Also with increasing number of hidden layers the AvgEER for CNNs does not change that much from 1 to 5 layers, it is around 11.55% for both number of units (512 or 1024). After 5 hidden layers the error for CNNs is gradually increasing and reaching near 12.15% for CNN_512 and CNN_1024 with 10 hidden layers. In general, the number of units in CNN models does not affect the error, the AvgEER approximately the same either for CNN_512 or CNN_1024, except for the CNN_1024 with 8 hidden layers. We suppose that this is occasional misleading result.

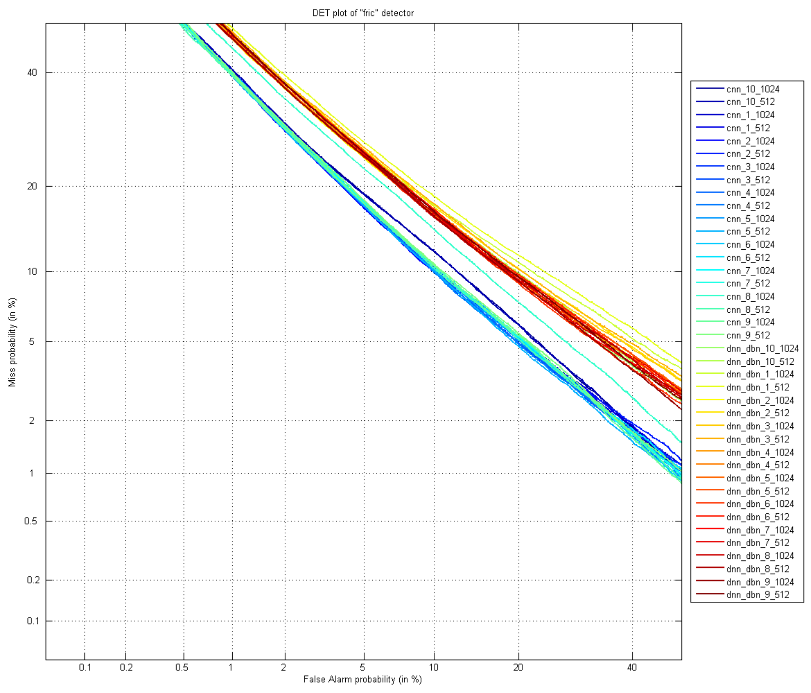

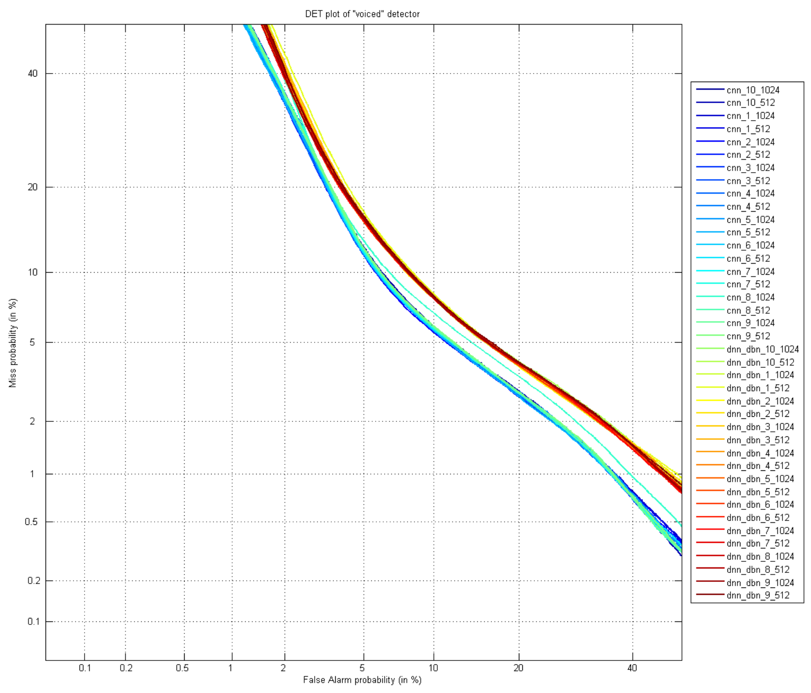

Figure 7.3: Detection Error Tradeoff of «fricative» and «voiced» as an example of manner detectors using different DNN topologies: CNN with 512 or 1024 hidden units along the hidden layers from 1 up to 10, the same variety of hidden layers and units for DBN-DNN.

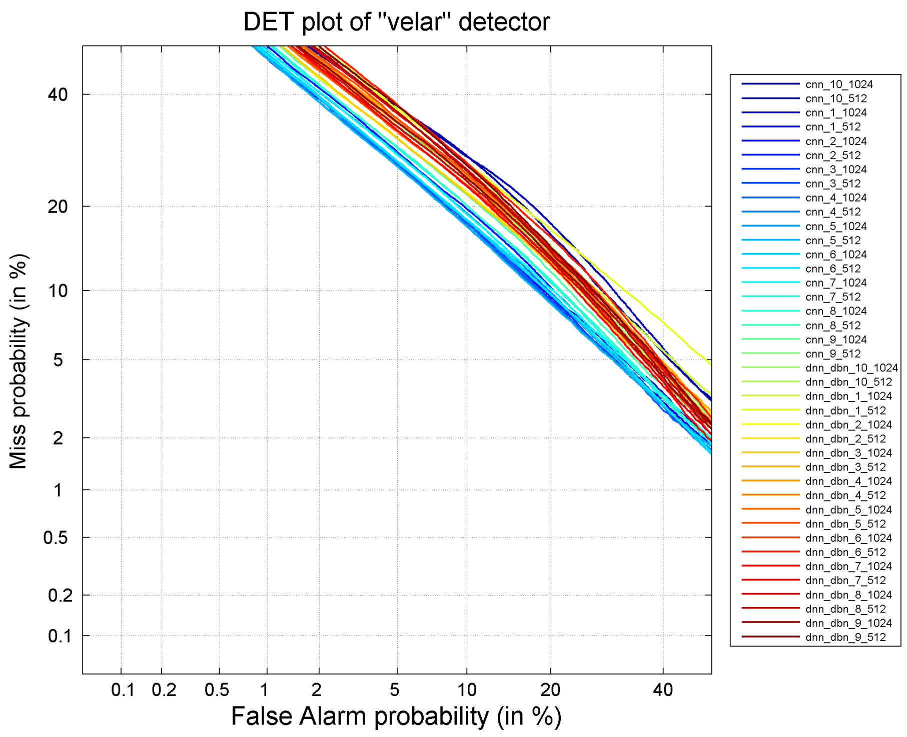

Figure 7.4: Detection Error Tradeoff of «velar» as an example of place detectors using different Deep Network topologies: CNN with 512 or 1024 hidden units along the hidden layers from 1 up to 10, the same variety of hidden layers and units for DBN-DNN.

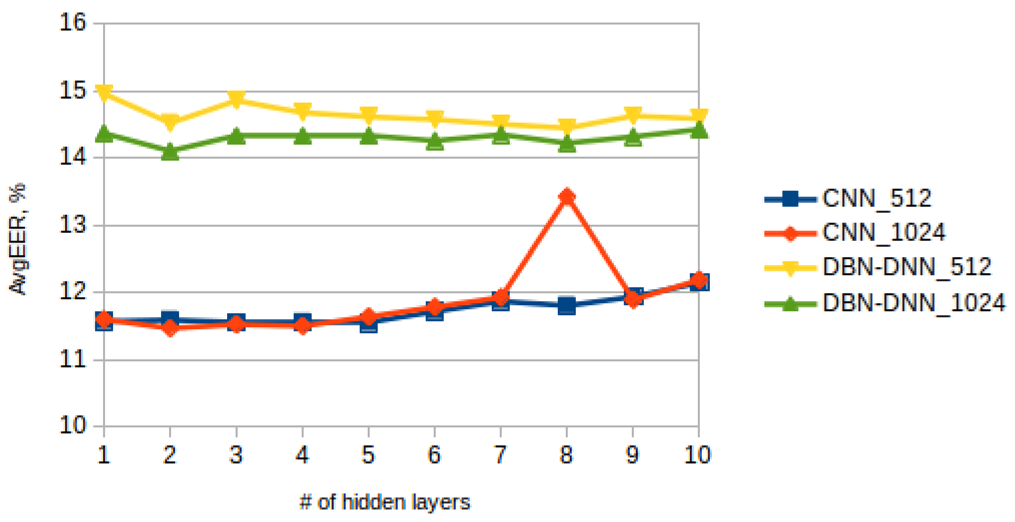

Figure 7.5: Average EER across all manner attribute detectors.

In case of the DBN models for manner detectors we see the opposite behavior (compare the CNNs): when the number of layers increase the error rate is gradually decreasing from 1 to 8 layers and after that increasing. There is clear gap between DBNs with 1024 and 512 units, the more number of units the better detector classify attributes. It can be noticed that DBN-DNN as well as CNNs models are stable, their errors vary within 1% or less.

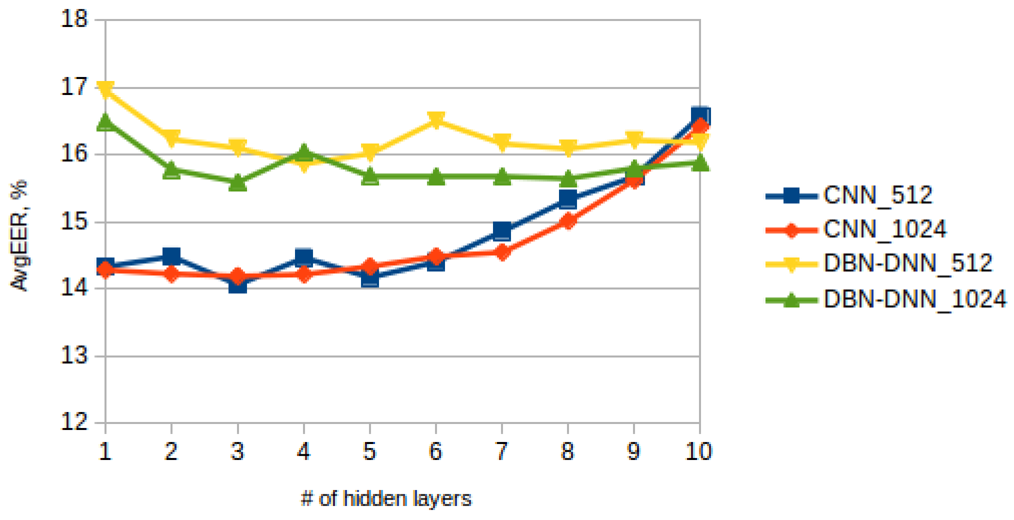

Figure 7.6: Average EER across all place attribute detectors.

In Figure 7.6 the AvgEER for place of articulatory detectors is plotted. The relation between CNNs and DBNs topologies remains the same as in manner case, i.e. the CNN models outperform the DBN across the whole range number of layers, except topology with 10 layers. The CNNs error rate for models with 1 up to 6 hidden layers fluctuates near 14.3%. The error of CNN topologies with more than 6 layers dramatically increases and reach a value of 16.58%. Similar to manners, the number of units in CNN models does not affect the error rate that much, it is hard to say which topology is better CNN_512 or CNN_1024, their AvgEERs are pretty close to each other. It is noticeable that DBNs with more units works better. It is clear positive tendency in DBN models: adding more hidden layers gradually improve the accuracy.

In Tables 7.1 and 7.2, we summarize the result DNN models of the articulatory attribute detectors, which show the lowest value of the AvgEER. Compare the performance of DNNs vs CNNs using DET plots and AvgEER, CNNs consistently outperform DNNs across different variety of tuned parameters; producing 18.8% relative error reduction for manner and

Table 7.1: Best models of manner detectors, which trained on OGI-TS corpus, with DBN-DNNs or CNNs with hidden layers from 1 up to 10 and 512 or 1024 units in each layer.

Topology	# of hid. layers	AvgEER, %
CNN_512	5	11.54
CNN_1024	2	**11.46**
DBN-DNN_512	8	14.45
DBN-DNN_1024	2	14.11

Table 7.2: Best models of place detectors, which trained on OGI-TS corpus, with DBN-DNNs or CNNs with hidden layers from 1 up to 10 and 512 or 1024 units in each layer.

Topology	# of hid. layers	AvgEER, %
CNN_512	3	**14.06**
CNN_1024	3	14.19
DBN-DNN_512	4	15.86
DBN-DNN_1024	8	15.65

10.3% for place compare with the best DBN-DNN models. This is consistent with our expectation that CNNs have better generalization ability than DNNs especially when the amount of training data are limited [46], this idea can be confirmed by the EER plots for every manner and place detector (see Appendix C).

7.2.3 Visualization of trained weights

Figure 7.7 shows several examples of the spectral filters (1-D convolutional kernels) learned by the convolutional layer of the CNN. The vertical dimension represent 8 weights of the convolutional kernel along the frequency axis, horizontal dimension represents 33 output neurons in the convolutional feature map. These filters look like 2-D Gabor filters [46] in varying directions: horizontal, vertical and diagonal filters.

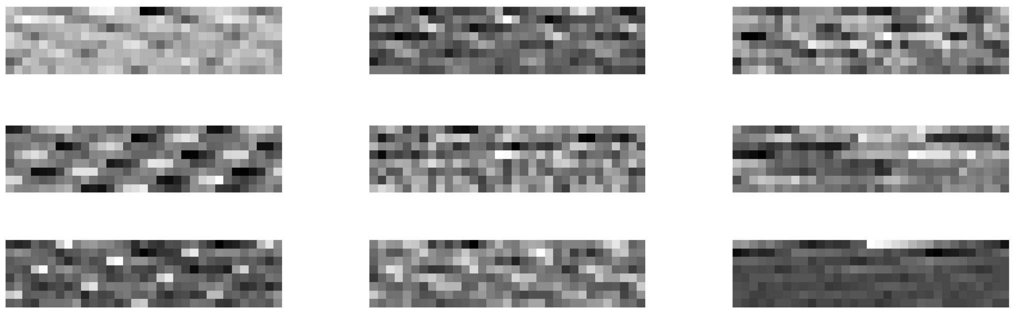

Figure 7.7: CNN spectral filters of size 8×33 learned by the convolutional layer.

In Figure 7.8 the DBN-DNN weights are depicted. These weights are trained by DBN-DNN with 2 hidden layers each of them has 1024 units. The weights, which are plotted, are connecting the last layer with 8 outputs and previous layer with 1024 units, thus we have 8 images of weights reshaped as 32×32 matrices. There is no such a clear structure on the images as for CNN filters, but these weight plots are used to visualize the convergence and anomaly of the training algorithm. If there are too much black or white pixels on the weight plots, it means that weights are very close to 0 or 1, i.e. too large or too small, that is not natural for DBN-DNN [92].

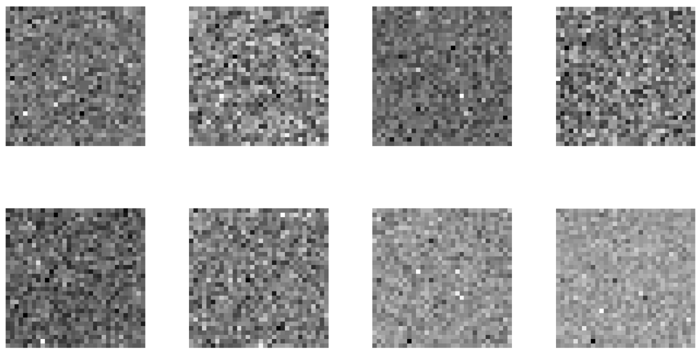

Figure 7.8: DBN-DNN weights between last layer with 8 units and previous layer with 1024 units. These are reshaped in 32×32 matrices.

CHAPTER 8

Conclusions

In this thesis it was proposed a promising model for speech attribute detection. Two models based on the cutting edge deep neural networks were compared. These are Convolutional Neural Networks (CNN) and feed-forward neural networks pre-trained with the stack of Restricted Boltzmann Machines (DBN-DNN). The proposed model is more related to the stochastic nature of the speech articulatory attributes, than that in paper [32]. Attribute detection can be considered as the multi-label detection problem, which was solved with the aid of our model. All experiments have been conducted on the multi-language OGI-TS speech dataset.

In order to find out the DNN model parameters for highest accuracy, many experiments have been conducted. The effect of number of hidden fully-connected layers and number of units were investigated. In order to measure the systems' performance on the test dataset and compare the models in general, several evaluation metrics were chosen. The DET curves approach in general and AvgEER (in Figures 7.5 and 7.6) in particular, consistently show that manner and place articulatory detectors trained with the CNN models work better than DBN-DNN models. The CNNs, compare with the DBN-DNNs, provide a significant error reduction producing 18.8% for manner and 10.3% for place relative AvgEER improvements (see Tables 7.1 and 7.2). Also tendency that CNNs outperform DBN-DNNs across different test parameters is confirmed by EER plots for every detector (see Appendix C). Moreover, manner speech features are detected more accurately then place features 11.46% versus 14.06% AvgEER, taking the best topologies.

The lowest AvgEER have been shown for manners by CNN with 2 hidden fully-connected layers each has 1024 units, for places the best results were obtained by CNN with 3 hidden layers and each of them had 512 units. Both CNN topologies has single convolutional and max-pulling layers.

From our experiments we can conclude that detectors trained with CNN models have better generalization ability than DBN-DNNs especially when the amount of training data is limited, as in our case we have very biased number of observations. It was shown (in Figure 7.7) that a CNN with random initialization can automatically learn various sets of edge detectors to locally extract low-level speech features. From the EER figures it can be concluded that CNN models suffer from overtraining, whenever we add more hidden fully-connected layers the error rate dramatically increases. In case of DBN-DNN we see the opposite behavior. Thus, we may conclude that stacking of RBMs or layer-wise pre-training gives gradual improvements of the model with the increase of hidden layers.

The next direction of the research is to apply multi-task learning approach as the inference framework above deep neural networks. Another investigation will be concerning the application of speech articulatory attributes in speaker recognition problem.

Bibliography

[1] The nobel prize in physiology or medicine 1906. nobelprize.org. nobel media ab 2014.

[2] Ossama Abdel-Hamid, Abdel rahman Mohamed, Hui Jiang, Li Deng, Gerald Penn, and Dong Yu. Convolutional neural networks for speech recognition. *IEEE/ACM TRANSACTIONS ON AUDIO, SPEECH, AND LANGUAGE PROCESSING*, October 2014.

[3] Ossama Abdel-Hamid, Abdel rahman Mohamed, Hui Jiang, and Gerald Penn. Applying convolutional neural networks concepts to hybrid NN-HMM model for speech recognition. In *2012 IEEE International Conference on Acoustics, Speech and Signal Processing (ICASSP)*. IEEE, mar 2012.

[4] P. Angkititrakul and J. H.L. Hansen. Advances in phone-based modeling for automatic accent classification. *Trans. Audio, Speech and Lang. Proc.*, 14(2):634–646, December 2006.

[5] Levent M. Arslan, John H. L. Hansen, Prof John, and H. L. Hansen. Language accent classification in american english, 1996.

[6] J. Baker, L. Deng, J. Glass, S. Khudanpur, C. H. Lee, N. Morgan, and D. O'Shgughnessy. Research developments and directions in speech recognition and understanding. *IEEE Signal Processing Magazine*, 26(3):75–80, 2009.

[7] Erwin H. Bareiss. Numerical solution of linear equations with toeplitz and vector toeplitz matrices. *Numer. Math.*, 13(5):404–424, oct 1969.

[8] Hamid Behravan, Ville Hautamauki, Sabato Marco Siniscalchi, Tomi Kinnunen, and Chin-Hui Lee. Introducing attribute features to foreign accent recognition. In *2014 IEEE International Conference on Acoustics, Speech and Signal Processing (ICASSP)*. Institute of Electrical & Electronics Engineers (IEEE), may 2014.

[9] Jacob Benesty, M. Mohan Sondhi, and Yiteng (Arden) Huang. *Springer Handbook of Speech Processing*. Springer-Verlag New York, Inc., Secaucus, NJ, USA, 2007.

[10] Y. Bengio. Learning deep architectures for AI. *Foundations and Trends® in Machine Learning*, 2(1):1–127, 2009.

[11] Y. Bengio, P. Lamblin, D. Popovici, and H. Larochelle. Greedy layer-wise training of deep networks. In *In NIPS*, 2007.

[12] Yoshua Bengio, Ian J. Goodfellow, and Aaron Courville. Deep learning. Book in preparation for MIT Press, 2015.

[13] Yoshua Bengio, Yann Lecun, and Yann Lecun. Convolutional networks for images, speech, and time-series, 1995.

[14] Christopher M. Bishop. *Pattern Recognition and Machine Learning*. Springer, 2006.

[15] Ronald Bracewell. *The Fourier Transform & Its Applications*. McGraw-Hill, 1965.

[16] Amy Brisben, Miguel Nicolelis, Mark Laubach, and Christopher Stambaugh. *Methods for Simultaneous Multisite Neural Ensemble Recordings in Behaving Primates*. Informa UK Limited, dec 1998.

[17] Niko Brummer. *Measuring, refining and calibrating speaker and language information extracted from speech*. PhD thesis, University of Stellenbosch, 2010.

[18] M. A. Carreira-Perpinan and G. E. Hinton. On contrastive divergence learning. *Proceedings of the Tenth International Workshop on Artificial Intelligence and Statistics (AISTATS'05)*, pages 33–40, 2005.

[19] M. A. Carreira-Perpinan and G. E. Hinton. *Proceedings of the Tenth International Workshop on Artificial Intelligence and Statistics, Jan 6-8, 2005, Savannah Hotel, Barbados*, chapter On Contrastive Divergence Learning, pages 33–40. 2005.

[20] A. H. Carter. *Classical and Statistical Thermodynamics*. Prentice Hall, New Jersey, 2001.

[21] A. Coates, H. Lee, and A. Y. Ng. An analysis of single-layer networks in unsupervised feature learning. *International Conference on Artificial Intelligence and Statistics (AISTATS)*, 2011.

[22] G. Cybenko. Approximations by superpositions of sigmoidal functions. *Mathematics of Control, Signals, and Systems*, 2(4):303–314, 1989.

[23] J. Dean. Large scale deep learning, April 2015. Available at `http://static.googleusercontent.com/media/research.google.com/ru//people/jeff/CIKM-keynote-Nov2014.pdf` [Online; accessed 9-June-2015].

[24] Li Deng. Three classes of deep learning architectures and their applications: A tutorial survey. *APSIPA Transactions on Signal and Information Processing*, 2012.

[25] Li Deng and Dong Yu. Deep learning: Methods and applications. *Found. Trends Signal Process.*, 7(3&#8211;4):197–387, June 2014.

[26] Dumitru Erhan, Pierre-Antoine Manzagol, Yoshua Bengio, Samy Bengio, and Pascal Vincent. The difficulty of training deep architectures and the effect of unsupervised pre-training. In *Twelfth International Conference on Artificial Intelligence and Statistics (AISTATS)*, pages 153–160, 2009.

[27] T. S. Ferguson. An inconsistent maximum likelihood estimate. *Journal of the American Statistical Association*, 77(380):831–834, 1982.

[28] Sadaoki Furui. *Digital speech processing, synthesis, and recognition*. Signal processing and communications. Marcel Dekker, New York, 2001.

[29] Silke Goronzy, Stefan Rapp, and Ralf Kompe. Generating non-native pronunciation variants for lexicon adaptation. *Speech Communication*, 42(1):109–123, jan 2004.

[30] Thomas Steele Hall. *Treatise of Man by Rene Descartes. French text with translation and commentary*. Harvard University Press, Cambridge, Massachusetts, 1972.

[31] John H.L. Hansen and Levent M. Arslan. Foreign accent classification using source generator based prosodic features. In *Proc. ICASSP*, pages 836–839. IEEE, 1995.

[32] V. Hautamaki, S. M. Siniscalchi, H. Behravan, V. M. Salerno, and I. Kukanov. Boosting universal speech attributes classification with deep neural network for foreign accent characterization. 2015.

[33] S. O. Haykin. *Neural Networks and Learning Machines*. 3 edition, 2008.

[34] Kaiming He, Xiangyu Zhang, Shaoqing Ren, and Jian Sun. Delving deep into rectifiers: Surpassing Human-Level performance on ImageNet classification, February 2015.

[35] Donald O. Hebb. *The Organization of Behavior*. New York: Wiley & Sons, 1949.

[36] G. Hinton. Deep belief network trained on mnist, example in action. Available at `http://www.cs.toronto.edu/~hinton/adi/index.htm` [Online; accessed 9-June-2015].

[37] G. Hinton. Deep belief networks. *Scholarpedia*, 4(5):5947, 2009.

[38] G. Hinton, P Dayan, B. Frey, and R. Neal. The "wake-sleep" algorithm for unsupervised neural networks. *Science*, 268(5214):1158–1161, may 1995.

[39] G. E. Hinton. Training products of experts by minimizing contrastive divergence. *Neural Computation*, 14(8):1771–1800, aug 2002.

[40] G. E. Hinton, S. Osindero, and Y. Teh. A fast learning algorithm for deep belief nets. *Neural Computation*, 18(7):1527–1554, 2006.

[41] G. E. Hinton and R. R. Salakhutdinov. Reducing the dimensionality of data with neural networks. *Science*, 313(5786):504–507, 2006.

[42] Geoffrey Hinton, Li Deng, Dong Yu, George Dahl, Abdel rahman Mohamed, Navdeep Jaitly, Andrew Senior, Vincent Vanhoucke, Patrick Nguyen, Tara Sainath, and Brian Kingsbury. Deep neural networks for acoustic modeling in speech recognition: The shared views of four research groups. *IEEE Signal Process. Mag.*, 29(6):82–97, nov 2012.

[43] Geoffrey E. Hinton. A practical guide to training restricted boltzmann machines. In Grégoire Montavon, Geneviève B. Orr, and Klaus-Robert Müller, editors, *Neural Networks: Tricks of the Trade*, volume 7700 of *LNCS*, chapter 24, pages 599–619. Springer Berlin Heidelberg, second ed. edition, 2012.

[44] S. Hochreiter. Untersuchungen zu dynamischen neuronalen netzen. Master's thesis, Institut f. Informatik, Technische Univ. Munich, 1991.

[45] S. Hochreiter, Y. Bengio, P. Frasconi, and J. Schmidhuber. Gradient flow in recurrent nets: the difficulty of learning long-term dependencies. *IEEE Press*, 2001.

[46] Jui-Ting Huang, Jinyu Li, and Yifan Gong. An analysis of convolutional neural networks for speech recognition. In *ICASSP*, April 2015.

[47] Sergey Ioffe and Christian Szegedy. Batch normalization: Accelerating deep network training by reducing internal covariate shift, March 2015.

[48] A. N. Kolmogorov. On the representation of continuous functions of many variables by superposition of continuous functions of one variable and addition. *Doklady Akademii Nauk SSSR*, 1957.

[49] L.D. Landau and E.M. Lifshitz. *Statistical Physics: Course of Theoretical Physics*, volume 5. Pergamon Press, Institute of Physical Problems USSR Academy of Sciences, 1969.

[50] H. Larochelle. Neural networks lectures, 2013. Available at `http://info.usherbrooke.ca/hlarochelle/cours/ift725_A2013/contenu.html` [Online; accessed 9-June-2015].

[51] H. Larochelle and Y. Bengio. Classification using discriminative restricted boltzmann machines. *Proceedings of the 25th international conference on Machine learning - ICML'08*, 2008.

[52] Y. LeCun, L. Bottou, G. B. Orr, and K.-R. Muller. Efficient backprop. *Neural Networks: tricks of the trade. - Springer*, 1998.

[53] Y. LeCun, S. Chopra, R. M. Hadsell, M.-A. Ranzato, and F.-J. Huang. *A tutorial on energy-based learning*. MIT Press, 2006.

[54] Y. LeCun, J. Denker, S. Solla, R. E. Howard, and L. D. Jackel. Optimal brain damage. *Advances in Neural Information Processing Systems II*, 1990.

[55] Y. LeCun and F. Huang. Loss functions for discriminative training of energy-based models. *Proceedings of the Tenth International Workshop on Artificial Intelligence and Statistics (AISTATS'05)*, 2005.

[56] Chin-Hui Lee and Sabato Marco Siniscalchi. An information-extraction approach to speech processing: Analysis, detection, verification, and recognition. *IEEE*, 101(5):1089–1115, 2013.

[57] J. Li, Y. Tsao, and Chin-Hui Lee. A study on knowledge source integration for candidate rescoring in automatic speech recognition. *ICASSP*, 2005.

[58] Jean luc Gauvain and Chin hui Lee. Maximum a posteriori estimation for multivariate gaussian mixture observations of markov chains. *IEEE Transactions on Speech and Audio Processing*, 2:291–298, 1994.

[59] Dau-Cheng Lyu, Sabato Marco Siniscalchi, Tae-Yoon Kim, and Chin-Hui Lee. Continuous phone recognition without target language training data. *ISCA*, 2008.

[60] A. Martin, G. Doddington, T. Kamm, M. Ordowski, and M. Przybocki. The det curve in assessment of detection task performance. pages 1895–1898, 1997.

[61] Warren S. McCulloch and Walter Pitts. A logical calculus of the ideas immanent in nervous activity. *The bulletin of mathematical biophysics*, 5:115–133, December 1943.

[62] Yajie Miao and Florian Metze. Improving low-resource cd-dnn-hmm using dropout and multilingual dnn training. In *INTERSPEECH'13*, pages 2237–2241, 2013.

[63] Marvin Minsky and Seymour Papert. *Perceptrons: an introduction to computational geometry*. The MIT Press, Cambridge MA, 1969.

[64] Y. K. Muthusamy, R. A. Cole, and B. T. Oshika. The OGI Multi-Language telephone speech corpus. In *Proceedings of the International Conference on Spoken Language Processing*, pages 895–898, 1992.

[65] Jinseok Nam, Jungi Kim, Eneldo Loza Mencía, Iryna Gurevych, and Johannes Fürnkranz. Large-scale multi-label text classification - revisiting neural networks. In Toon Calders, Floriana Esposito, Eyke Hüllermeier, and Rosa Meo, editors, *Proceedings of the European Conference on Machine Learning and Principles and Practice of Knowledge Discovery in Databases (ECML-PKDD-14), Part 2*, volume 8725 of *Lecture Notes in Computer Science*, pages 437–452. Springer Berlin Heidelberg, 2014.

[66] John Nerbonne. Linguistic variation and computation (invited talk). In *EACL*, pages 3–10. The Association for Computer Linguistics, 2003.

[67] M. A. Nielsen. *Neural Networks and Deep Learning*. Determination Press, 2015.

[68] M. Ranzato, Y. Boureau, S. Chopra, and Y. LeCun. A unified energy-based framework for unsupervised learning. *Proceedings of the Eleventh International Conference on Artificial Intelligence and Statistics (AISTATS'07)*, 2007.

[69] Marc'Aurelio Ranzato, Christopher Poultney, Sumit Chopra, and Yann Lecun. Efficient learning of sparse representations with an energy-based model. In *Advances in Neural Information Processing Systems (NIPS 2006*, 2006.

[70] Frank Rosenblatt. The perceptron - a perceiving and recognizing automaton. Technical Report 85-460-1, Cornell Aeronautical Laboratory, 1957.

[71] D.E. Rumelhart, G.E. Hinton, and R. J. Williams. Learning internal representations by error propagation. *Parallel distributed processing: Explorations in the microstructure of cognition*, 1, 1986.

[72] Tara N. Sainath, Brian Kingsbury, Abdel-rahman Mohamed, George E. Dahl, George Saon, Hagen Soltau, Tomás Beran, Aleksandr Y. Aravkin, and Bhuvana Ramabhadran. Improvements to deep convolutional neural networks for LVCSR. In *2013 IEEE Workshop on Automatic Speech Recognition and Understanding, Olomouc, Czech Republic, December 8-12, 2013*, pages 315–320, 2013.

[73] Tara N. Sainath, Abdel-rahman Mohamed, Brian Kingsbury, and Bhuvana Ramabhadran. Deep convolutional neural networks for LVCSR. In *IEEE International Conference on Acoustics, Speech and Signal Processing, ICASSP 2013, Vancouver, BC, Canada, May 26-31, 2013*, pages 8614–8618, 2013.

[74] R. Salakhutdinov and G. Hinton. Replicated softmax: an undirected topic model. *Neural Information Processing Systems*, 23, 2010.

[75] R. Salakhutdinov, A. Mnih, and G. Hinton. Restricted boltzmann machines for collaborative filtering. *Proceedings of the 24th international conference on Machine learning - ICML'07*, 2007.

[76] Frank Seide, Gang Li, and Dong Yu. Conversational speech transcription using context-dependent deep neural networks. In *Interspeech 2011*. International Speech Communication Association, August 2011.

[77] S. M. Siniscalchi, Dau-Cheng Lyu, T. Svendsen, and Chin-Hui Lee. Experiments on Cross-Language attribute detection and phone recognition with minimal Target-Specific training data. *Audio, Speech, and Language Processing, IEEE Transactions on*, 20(3):875–887, March 2012.

[78] Sabato M. Siniscalchi, Jeremy Reed, Torbjørn Svendsen, and Chin-Hui Lee. Universal attribute characterization of spoken languages for automatic spoken language recognition. *Computer Speech & Language*, 27(1):209–227, January 2013.

[79] Sabato Marco Siniscalchi, Torbjorn Svendsen, and Chin-Hui Lee. Towards bottom-up continuous phone recognition. *ASRU*, 2007.

[80] Sabato Marco Siniscalchi, Torbjorn Svendsen, and Chin-Hui Lee. Toward a detector-based universal phone recognition. *IEEE*, 2008.

[81] P. Smolensky. Chapter 6: Information processing in dynamical systems: Foundations of harmony theory. *Parallel Distributed Processing: Explorations in the Microstructure of Cognition*, 1:194–281, 1986.

[82] P. Smolensky. Information processing in dynamical systems: Foundations of harmony theory. *Parallel Distributed Processing: Explorations in the Microstructure of Cognition*, 1986.

[83] Bennie G. Thompson. Border security fraud risks complicate states ability to manage diversity visa program. *GAO*, 2007.

[84] R. C. Tolman. *The Principles of Statistical Mechanics*. Dover Publications, 1938.

[85] Yukio Tono, Yuji Kawaguchi, and Makoto Minegishi, editors. *Developmental and Crosslinguistic Perspectives in Learner Corpus Research*. Tokyo University of Foreign Studies 4. John Benjamins, Philadelphia, 2012.

[86] Pascal Vincent, Hugo Larochelle, Yoshua Bengio, and Pierre A. Manzagol. Extracting and composing robust features with denoising autoencoders. In *Proceedings of the 25th International Conference on Machine Learning*, ICML '08, pages 1096–1103, New York, NY, USA, 2008. ACM.

[87] K.V. Voroncov. Lekcii po nejronnim setiam. 2007.

[88] Huazheng Wang, Bin Gao, Jiang Bian, Fei Tian, and Tie-Yan Liu. Solving verbal comprehension questions in IQ test by Knowledge-Powered word embedding, May 2015.

[89] Wikipedia. Canonical ensemble — wikipedia, the free encyclopedia, 2015. Available at `http://en.wikipedia.org/w/index.php?title=Canonical_ensemble&oldid=659866755` [Online; accessed 9-June-2015].

[90] Wikipedia. Neuron — wikipedia, the free encyclopedia, 2015. Available at `http://en.wikipedia.org/w/index.php?title=Neuron&oldid=664941774` [Online; accessed 9-June-2015].

[91] Yong Xu, Jun Du, Li-Rong Dai, and Chin-Hui Lee. A regression approach to speech enhancement based on deep neural networks. *IEEE/ACM Trans. Audio, Speech and Lang. Proc.*, 23(1):7–19, January 2015.

[92] Jason Yosinski and Hod Lipson. Visually debugging restricted boltzmann machine training with a 3d example. In *The Representation Learning Workshop, 29-th International Conference on Machine Learning, Edinburgh, Scotland, UK*, 2012.

[93] D. Yu and L. Deng. *Automatic Speech Recognition: A Deep Learning Approach*. Springer, London, 2015.

[94] Min-Ling Zhang. Multilabel neural networks with applications to functional genomics and text categorization. *IEEE Transactions on Knowledge and Data Engineering*, 18(10):1338–1351, October 2006.

APPENDIX A

Manner Multi Labels mapping to Phonemes

```
—— SPANISH ——
fric ch f hh hs hx jh s sh th
fric_voiced bx dh gx
gs_voiced l ly r w y
nasal_voiced m n ng
sil pau
stop k p t
stop_voiced b d g
voiced_vowel aa ae ah ay eh ey ih iy ow uh uw

—— ENGLISH ——
fric ch f hh s sh th
fric_voiced dh jh v z
gs_voiced l r w y
nasal_voiced m n ng
sil pau
stop k p t
stop_voiced b d dx g
voiced_vowel aa ae ah aw ay eh er ey ih iy ow oy uh uw

—— HINDI ——
fric ch chh f hh s sh
fric_voiced jh z
```

```
gs_voiced l r w y
nasal_voiced m n ng
sil ddcl dtcl pau
stop dt dth dx k kh p rd t th
stop_voiced b bh d dd dh g
voiced_vowel a aa ae ah ai aw e eh ih iy ow uh uw
```

—— GERMAN ——

```
fric ch cx f hh s sh ts x
fric_voiced jh v z
gs_voiced l r y
nasal_voiced m n ng
sil pau
stop dx k p t
stop_voiced b d g
voiced_vowel A: a aa ae ah ai aw ea ee eh ia ih ihw iy oa oo uh uw
```

—— MANDARIN ——

```
fric c ch f hh s sh shr ts tsh tsr
fric_sil chcl tscl tsrcl
fric_voiced v
gs_voiced l r w
nasal_voiced m n ng
sil pau
stop k kh p ph t tH
voiced_vowel a aa ae ah ai aw eh er ey ih iy iyw oe ow ox u uw
```

—— JAPANESE ——

```
fric ch f hh s sh ts
fric_voiced dz jh z
gs_voiced rrr w y
nasal_voiced m n ng
sil pau
stop k p t
stop_voiced b d g
```

```
voiced_vowel a ah ay ey iy ow uw
```

APPENDIX B

Place Multi Labels mapping to Phonemes

```
——- SPANISH ——-
coronal r
coronal_dental d l n s t
coronal_dental_glottal hs
dental dh th
glottal hh
high ch ih iy jh sh uh uw y
labial b bx f m p w
low aa ae ay
mid ah eh ey ow
sil pau
velar g gx hx k ng

——- ENGLISH ——-
coronal d dx l n s t z
dental dh th
glottal hh
high ch ih iy jh sh uh uw y
labial b f m p v w
low aa ae aw ay oy
mid ah eh ey ow
sil pau
velar g k ng
```

```
---- HINDI ----
coronal d dd dx l s z
coronal_dental dt dth n
coronal_high ch chh jh
glottal hh
high ih iy sh uh uw y
labial b bh f m p w
low a aa ae ai aw
mid ah eh ow
sil ddcl dtcl pau
velar g k kh ng

---- GERMAN ----
coronal ch cx d dx l n r s t ts x z
coronal_glottal hh
coronal_high jh sh y
coronal_sil pau
dental_labial f v
high ih iy uw
high_mid uh
labial b m p
low A: a aa ae
mid ah ee eh oa oo
velar g k ng

---- MANDARIN ----
coronal l n
coronal_dental s t
dental tH
glottal hh
high ch ih iy iyw sh shr uw
labial f m p ph v w
low aa ae aw
mid ah eh er ey oe ow ox
```

```
sil chcl pau tscl tsrcl
velar k kh ng
```

––– JAPANESE –––

```
coronal_dental d dz n s t ts z
coronal_high ch jh sh y
glottal hh
high iy uw
labial b f m p w
low a ay
mid ah ey ow
sil pau
velar g k ng
```

APPENDIX C

Equal Error Rate for all detectors and different Neural Network topologies

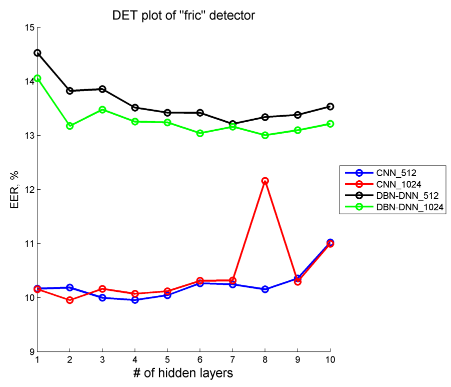

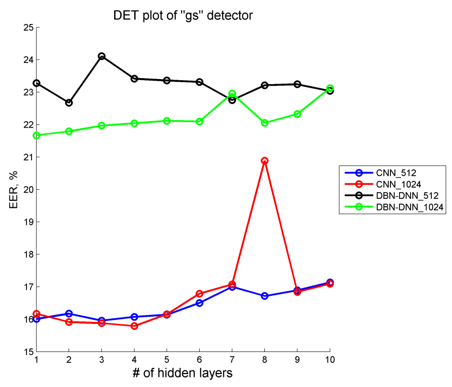

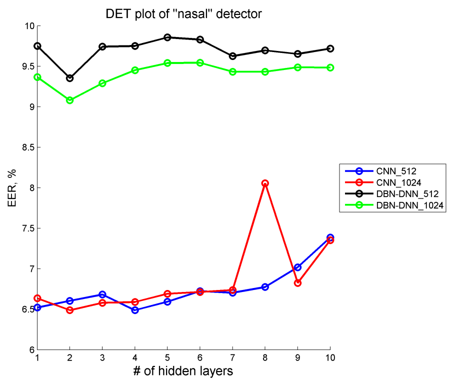

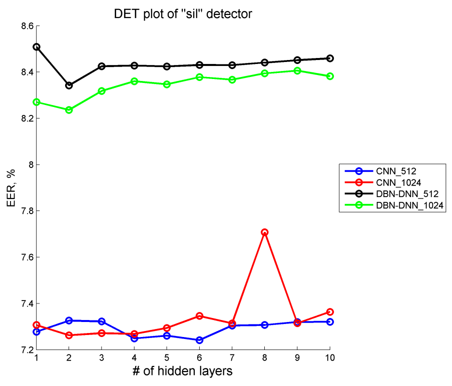

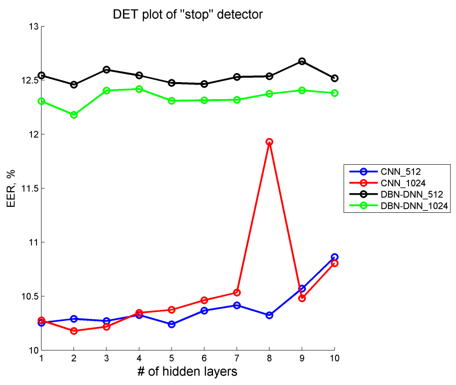
DET plot of "stop" detector
EER, %
# of hidden layers
CNN_512
CNN_1024
DBN-DNN_512
DBN-DNN_1024

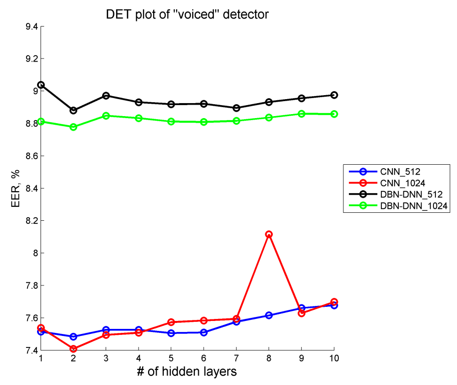
DET plot of "voiced" detector
EER, %
# of hidden layers
CNN_512
CNN_1024
DBN-DNN_512
DBN-DNN_1024

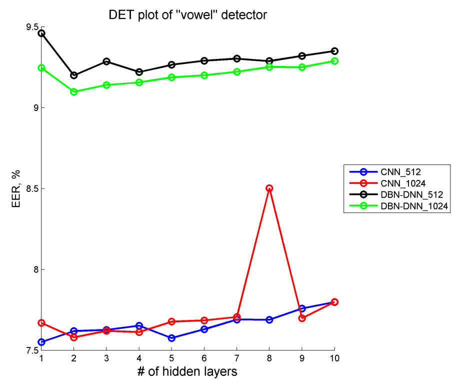
DET plot of "vowel" detector
EER, %
# of hidden layers
CNN_512
CNN_1024
DBN-DNN_512
DBN-DNN_1024

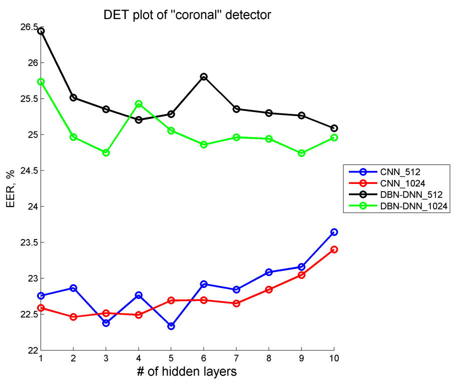
DET plot of "coronal" detector
EER, %
# of hidden layers
CNN_512
CNN_1024
DBN-DNN_512
DBN-DNN_1024

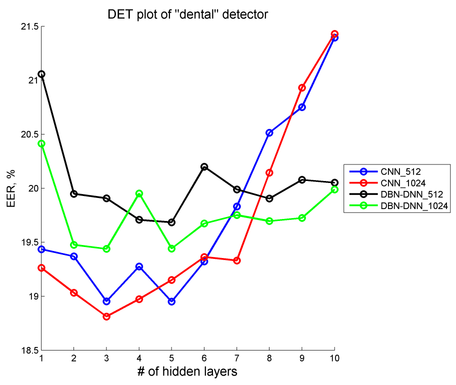
DET plot of "dental" detector
EER, %
# of hidden layers
CNN_512
CNN_1024
DBN-DNN_512
DBN-DNN_1024

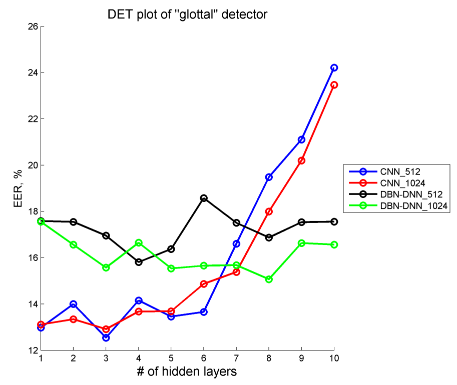
DET plot of "glottal" detector
EER, %
# of hidden layers
CNN_512
CNN_1024
DBN-DNN_512
DBN-DNN_1024

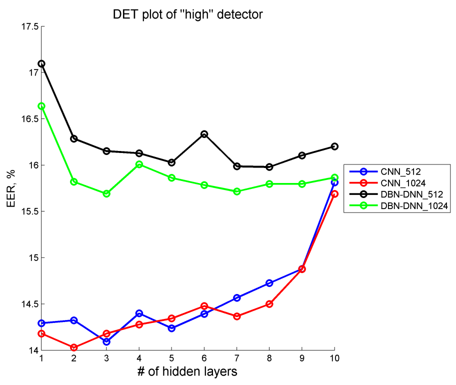
DET plot of "high" detector
EER, %
# of hidden layers
CNN_512
CNN_1024
DBN-DNN_512
DBN-DNN_1024

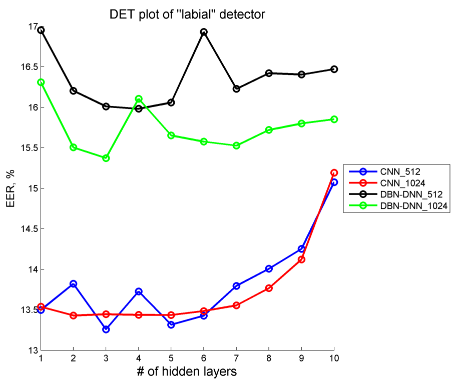
DET plot of "labial" detector
EER, %
# of hidden layers
CNN_512
CNN_1024
DBN-DNN_512
DBN-DNN_1024

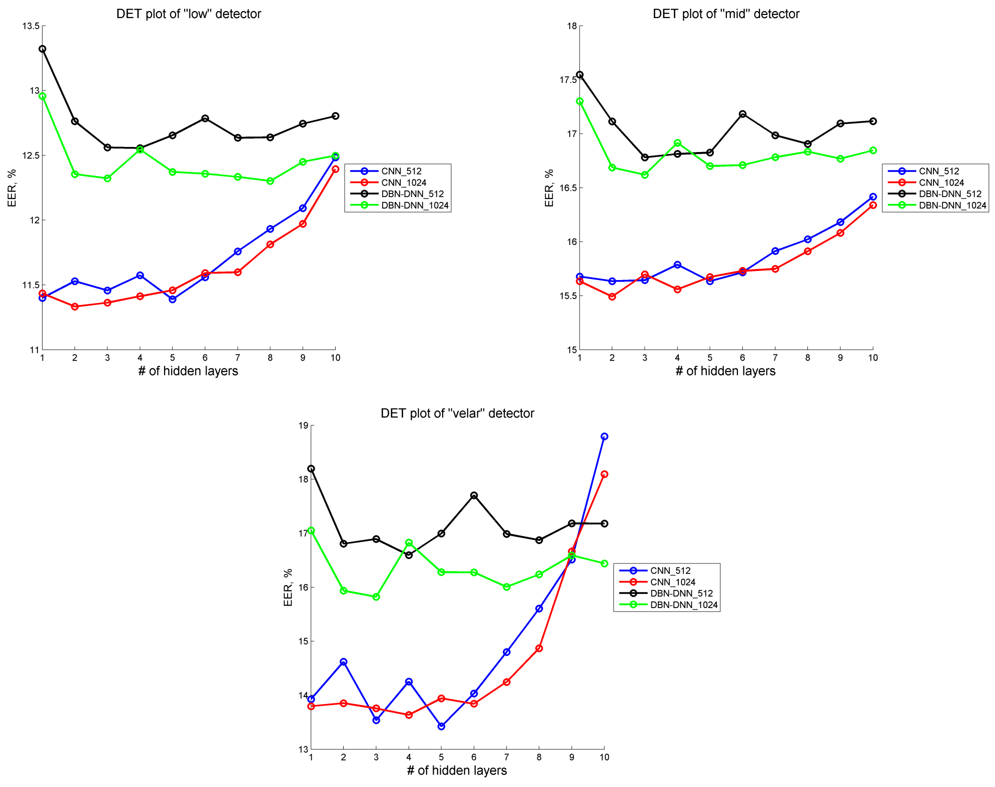

Figure C.1: EER for every articulatory detector depends on variety of DBN-DNN and CNN models: from 1 up to 10 hidden layers and each of them with 512 or 1024 units.